

Master's Thesis

Effects of High CO₂ on Immune Response and Scale Structures in Juvenile Turbot (*Scophthalmus maximus*)



By

Huajing Yan

Thesis Advisors

Prof. Thorsten Reusch (Evolutionary Ecology of Marine Fishes, GEOMAR)

Prof. Stanislav Gorb (Functional Morphology and Biomechanics, Zoological Institute, CAU)

Joanna Miest (Evolutionary Ecology of Marine Fishes, GEOMAR)

Marlene Spinner (Functional Morphology and Biomechanics, Zoological Institute, CAU)

Catriona Clemmesen-Bockelmann (Evolutionary Ecology of Marine Fishes, GEOMAR)

May 2016

TABLE OF CONTENTS

Abstract.....	1
1. Introduction	3
2. Materials & Methods	7
2.1 Animals.....	7
2.2 Experimental Set Up.....	8
2.3 Water Analysis.....	10
2.4 Sampling	10
2.5 Flow Cytometry.....	11
2.6 Lysozyme Activity	11
2.7 Molecular Genetic Analysis.....	12
2.7.1 RNA Extraction & cDNA Synthesis.....	12
2.7.2 Primers	13
2.7.3 Gene Expression Analysis using qPCR	14
2.7.4 Gene Expression Analysis using the Fluidigm Biomark System	15
2.8 Turbot Scale Mechanical Property Analysis	16
2.9 Statistical Analysis	17
3. Results	18
3.1 Water Properties	18
3.2 Growth & Condition.....	20
3.3 Lysozyme Activity	22
3.4 Gene Expression	24
Treatment Effect.....	24
Time Effect.....	29
3.5 Blood Count	30
3.6 Scale Mechanical Properties	32
4. Discussion	35
4.1 Water Properties	35
4.2 Growth.....	36
4.3 Short Term Study (Acute CO ₂)	36
4.4 Long Term Study (Chronic CO ₂)	40
5. Conclusion.....	46
Acknowledgement.....	47
References	49
Appendix	57
Declaration Of Authorship.....	61

ABSTRACT

Ocean acidification (OA), a consequence of the dissolution of excess anthropogenic carbon dioxide in ocean water, is ongoing worldwide. Possible effects of ocean acidification on marine organisms include impacts on growth and development, survival, reproduction, acid-base regulation, behavior, and biomineralizing species calcification rates. The health and well-being of organisms depends on their immune system, therefore one part of this thesis was to study the effect of ocean acidification on the immunity. Another part is in regards to the effect of ocean acidification on biomineralization; in this thesis is fish with biomineralizing scales, which could also influence the health of an organism. Early life stages are highly vulnerable; therefore this thesis studied juvenile turbot (*Scophthalmus maximus*) response to the effects of elevated carbon dioxide (CO₂) levels on the innate immune system and scale structures. Turbots were exposed to three different levels of CO₂ (ambient, 1000 μatm and 2000 μatm) in both short term (1 week) and long term (16 weeks) exposure. In the short term experiment, a stress response in the highest CO₂ treatment was observed, evident from an increase in lysozyme activity which led to a downregulation of an antimicrobial peptide (*hepcidin1*). No CO₂ effect was found in the long term experiment on both the immune response and scale structure, suggesting the ability of turbot to acclimate to future predicted oceanic CO₂ levels. However changes in gene expression and lysozyme activity in the long term experiment suggested a stress effect from seasonal temperature variations.

1. INTRODUCTION

Industrialization and human population growth has resulted in increased use of fossil fuels, deforestation, and cement production which has caused a great increase of carbon dioxide CO₂, the primary greenhouse gas, in the atmosphere (Caldeira & Wickett, 2003). Atmospheric gas and dissolved oceanic gas are in equilibrium, therefore, oceans act as a major sink for atmospheric CO₂ and the increase in CO₂ in the atmosphere has led to an increase in the ocean CO₂ (Levine & Doney, 2006). The Intergovernmental Panel on Climate Change (IPCC) predicts that the global mean oceanic CO₂ values are expected to reach 1,000 ppm CO₂ by year 2100, causing a pH decrease of 0.3-0.4 (IPCC, 2014), and could reach 1,900 ppm CO₂ by year 2300 (Caldeira & Wickett, 2003; IPCC, 2007). However, many coastal regions around the world are already seeing levels of CO₂ that match global predictions beyond year 2100 (Melzner et al., 2013).

The carbonate system in the ocean consists of dissolved CO₂, HCO₃⁻, and CO₃²⁻ which are at chemical equilibrium (Dickson et al., 2007). An increase in CO₂ therefore leads to an increase in HCO₃⁻ and decreases in CO₃²⁻, with also an increase in H⁺ (hydrogen ions), resulting in the disturbance of the entire carbonate system with a decrease in pH causing ocean acidification.

Ocean acidification has many consequences on marine organisms. Calcifying organisms are particularly affected (Riebesell et al., 2000). Many studies on species with calcium carbonate skeletons such as calcifying phytoplankton, molluscs, crustaceans, and echinoderms have shown that acidification has caused reduced rates of calcification and significant shell dissolution in these organisms (Riebesell et al., 2000; Feely et al., 2004). The formation of biogenic calcium carbonate (CaCO₃) which is a key building component for many organisms that form shells or plates (Hernroth et al., 2012) is decreased or even prevented under low ocean pH. For the formation of calcium carbonate, calcium ions (Ca²⁺) and carbonate ions (CO₃²⁻) which are both present in seawater are combined together by these organisms. When ocean acidification occurs, an increase of CO₂ reacting with H₂O causes an increase of hydrogen ions (H⁺) which bind to carbonate ions with greater attraction than calcium ions (Fabry et al., 2008). When this occurs, shell-forming organisms can no longer use the carbonate ions to form new shells or skeletons and if there are more hydrogen ions than free carbonate ions,

this could even lead to shell dissolution when the hydrogen ions start breaking down carbonate from existing shells and skeletons (Guinotte & Fabry, 2008).

However, not only shelled organisms are impacted by ocean acidification. Studies on fish have shown physiological changes due to increased CO₂ such as changes in growth, organ development, reproduction, larval development, or behavior (Frommel et al., 2011; Frommel et al., 2014; Heuer & Grosell, 2014; Ishimatsu et al., 2004; Munday et al., 2014). Compensatory internal acid-base regulation is hypothesized to be responsible for these physiological and behavioral alterations (Heuer & Grosell, 2014). To ensure homeostasis and acid-base stability, regulation of ion transporting proteins such as *NHE* or *V-type H⁺-ATPase* can be modified to compensate for the change of internal pH levels (Souza et al., 2014; Gilmour & Perry, 2009).

Since internal regulation is costly, other physical functions have to be compromised in order to survive in a high CO₂ environment; therefore it is believed that fish's immune system could also be affected by this regulation for survival. It has been seen in studies on invertebrates such as the green sea urchin (*Strongylocentrotus droebachiensis*), a sea star (*Leptasterias polaris*), the blue mussel (*Mytilus edulis*), and the Norway lobster (*Nephrops norvegicus*) that their immune responses have been impacted due to ocean acidification (Bibby et al., 2008; Dupont & Thorndyke 2012; Hernroth et al., 2012). However, no knowledge is yet available on the impact of high CO₂ on vertebrate immune system response.

The fish immune system is physiologically similar to higher vertebrates and consists of the innate and adaptive immune system (Uribe et al., 2011). The innate immune system consists of proteins and cells that are always present but nonspecific and the adaptive immune system, which is specific, is activated when the pathogen passes the innate immune system. The difference between fish and higher vertebrates is that in fish the nonspecific immunity is the fundamental defense mechanism due to limitations of the adaptive immune system (Uribe et al., 2011). Various factors can influence the innate immune response such as temperature, light, water quality, salinity, stress, or food additives (Uribe et al., 2011).

The fish used in this experiment, turbot (*Scophthalmus maximus*) is a highly prized flatfish and one of the most commercially important fish in aquaculture (Zhang et al., 2011). It is distributed along the coast of Europe in the Northeast Atlantic, Mediterranean Sea, Baltic Sea, up until the Norwegian Sea (Exadactylos et al., 2007). Turbot are abundant in coastal waters with shallow soft bottom habitats and feed on crustaceans and fish (Froese & Pauly, 2015) and have been known to grow up to 100 cm long and weigh 25 kg (Exadactylos et al., 2007).

Turbot, and other flatfish, have modified elasmoid scales called tubercles on their skin (Faílde et al., 2014). These tubercles are small, isolated, mineralized conical plates randomly distributed in the pigmented side of the body which originate from thin and flat plates located in the skin of larvae and juveniles, whose structure is that of regular-developing elasmoid scales (Zylberberg et al., 2003; Murcia et al., 2015). Since these tubercles undergo biomineralization like the shells of shelled organisms, and are partly exposed to the water, ocean acidification could also affect the growth process and material properties of these modified scales and influence the health of the fish.

Apart from studies showing that elevated CO₂ can alter calcification rates or carbonate dissolution, it could also impact the structure of the calcifying skeleton itself. Studies by Gutowska (2010) showed that cuttlebone from cephalopod *Sepia officinalis*, which consists of aragonite (CaCO₃) and undergoes biomineralization, experienced changes in mineralized structures under elevated CO₂. Since turbot scales also consists of mineralizing materials, ocean acidification could also impact the fundamental structure of the tubercle scale itself, therefore altering the mechanical properties of the scale.

In this study, a short term experiment of 1 week and a long term of 16 weeks were performed. Heuer & Grosell (2014) mentioned in their paper that “abrupt and relatively short-term CO₂ exposures are inherently limiting in their ability to assess the adaptive capacity of a species” and a study by Stiller et al., (2015) found that turbot in their studies could acclimatize to hypercapnic conditions after two weeks. Therefore an experiment investigating an acute and chronic exposure can provide knowledge into the response of turbot immune responses to ocean acidification and possible acclimation.

Early life stages of fish are found to be less tolerant than adult life stages to environmental toxicity (Hutchinson et al., 1998) and high juvenile mortality have been observed in marine invertebrates (Gosselin & Qian, 1997), therefore juvenile turbot were used in this study. We studied the effect of two levels of elevated CO₂, ~1000 µatm from end of century predictions and ~2000 µatm from year 2300 predictions, on the innate immune system and tubercle scale properties of juvenile turbot. The innate immune system parameters that were measured were lysozyme activity, blood cell composition, and immune gene expression. Adaptive immune genes were also analyzed for a full immune response picture along with other non-immunity genes to provide a better understanding of any effects found from innate immune gene response. The scale properties were measured by nanoindentation on turbot tubercles.

Nanoindentation methods used in this experiment followed methods developed by Oliver and Pharr (1992;2004), which measured hardness and elastic modulus of a material by indentation at nanometer scales. Oliver and Pharr's method can determine mechanical properties of small-sized materials such as thin films and small structural features, which could be obtained directly from indentation load-displacement measurements.

The hypotheses to be tested within this study are that:

1. Increased CO₂ has an effect on the immune system gene expression in dependence of treatment time.
2. Increased CO₂ effects biomineralization of the fish scale, resulting in altered mechanical properties.

2. MATERIALS & METHODS

2.1 ANIMALS

The experiment was conducted in two parts, a short term experiment of 1 week, and a long term experiment lasting 16 weeks.

Juvenile turbot (*Scophthalmus maximus*) were acquired from Stolt Sea Farm in Norway in 2014. They were reared in GEOMAR's NEMO Hall with flow through Baltic Sea water at ambient conditions prior to the experiment. At the beginning of the short term experiment, the turbot weighed 170.8 ± 5.2 g and measured 20.4 ± 0.2 cm in length (head-tail length). In the long term study, the turbot weighed 126.1 ± 3.3 g and had a length of 18.5 ± 0.2 cm at the start experiment.

In the short term experiment, all fish were fed with turbot feed from Skretting (R-3 Europa 22%) every morning at 0.2% of fish body weight. Fish from the long term experiment were fed with the same type of food every morning, however the amount was adjusted every week to 0.5% of the average fish weight per each tank. In both experiments, fish were kept on a restrictive diet following values from Sæther and Jobling (1999). All food was eaten and all the tanks were cleaned daily.

In order to allow individual analysis of the fish in the long term experiment each animal received a colour tag on their dorsal fin.

2.2 EXPERIMENTAL SET UP

The experiment consisted of a short term 1 week experiment and a long term 16 week experiment. Both experiments consisted of 3 treatments: ambient CO₂ (i.e control), medium CO₂ (approx. 1000 µatm), and high CO₂ (approx. 2000 µatm). All treatments were run with 4 replicate tanks each and each tank contained 3 turbot totaling 12 tanks and 36 turbot for each experiment (Fig. 1).



Figure 1: Experimental set up of both studies

The experimental tanks were 60 L in volume, with continuous flow through Baltic water from the Kiel Fjord at a flow rate of 400 ml/min. These tanks rested in a large holding tank filled with Baltic Sea water. Additionally each tank was fitted with a filter and a protein skimmer while the CO₂ treated tanks also contained a CO₂ tube and pH probe connected to a computer system (Fig. 2).

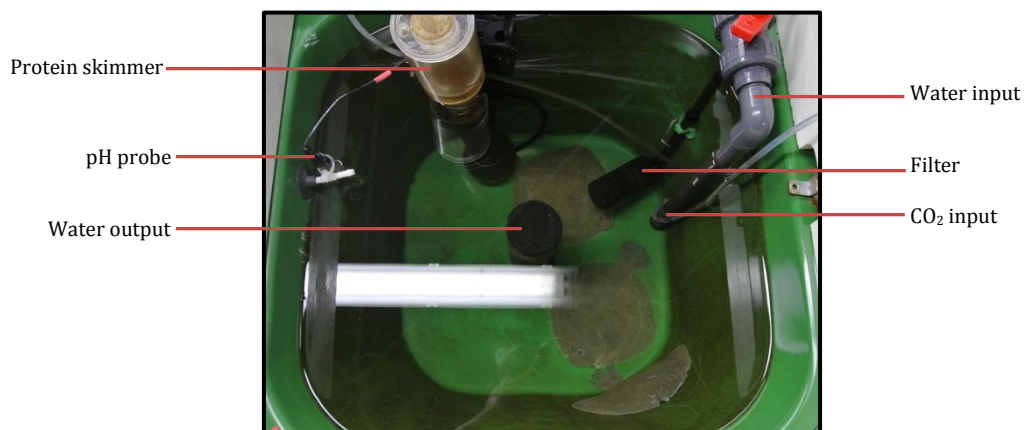


Figure 2: Equipment in each tank

The iks aquastar computer system (iks ComputerSysteme GmbH, Germany) was used to monitor the pH levels in each tank (Fig. 3). Each CO₂-treated tank had a pH probe and CO₂ tube connected to the iks system. The target pH value for each tank was programmed into the system controlling the CO₂ valve in order to maintain the targeted pH value.



Figure 3: iks aquastar computer system used for pH monitoring

The water temperature in the experimental tanks varied with the water temperature of the Fjord but was kept at 20°C maximum through the hall's air condition system and the large water body of the holding tanks. Light intensity was set to approximately 30 lux with an interval of 11:13 light: dark. The pH, salinity, and temperature of each tank were monitored daily. The pH was measured with a pH Electrode (SenTix 81, Wissenschaftlich-Technische Werkstätten GmbH, Germany) calibrated with NBS buffer while salinity and temperature were measured with a conductivity probe (TetraCon 325 and Multi 350i, Wissenschaftlich-Technische Werkstätten GmbH, Germany). Water quality was checked periodically by measuring dissolved oxygen with an oxygen probe (CellOx 325, Wissenschaftlich-Technische Werkstätten GmbH, Germany), measuring ammonium with Tetra Test NH₃/NH₄⁺ kit (Spectrum Brands, Inc. USA), and measuring nitrite with Tetra Test NO₂ kit (Spectrum Brands, Inc. USA).

2.3 WATER ANALYSIS

Water samples were taken weekly by filling and overflowing the bottles with a plastic tube from the tank into the bottom of the sample bottle. This avoids air bubbles and washes out the bottles. All samples were immediately poisoned with a saturated HgCl₂ solution (0.5 ‰ final concentration) for storage. Samples for total alkalinity (TA) measurements were stored in plastic bottles and dissolved inorganic carbon (DIC) samples were stored in airtight glass bottles at room temperature.

Total alkalinity of the water samples was analyzed with Metrohm 862 Compact Titrosampler and the results were calculated with MATLAB script supplied by Kai Schulz, GEOMAR, Kiel, Germany (2005) and DIC was measured using an AIRICA system (Marianda) via a LI-COR 7000 infrared CO₂/H₂O analyser. Both TA and DIC values were then corrected using the Dickson seawater standard as reference material. The pCO₂ was calculated from measured DIC and pH values using CO2SYS software (Pierrot et al. 2006) with dissociation constants from Mehrbach et al. (1973) as refitted by Dickson and Millero (1987) and KHSO₄ dissociation constant after Dickson (1990).

2.4 SAMPLING

In the long term exposure, all fish were weighed, measured and 100 µl of blood was taken from the caudal vein with a 0.4 x 19 mm (Nr. 20) needle and 1 ml syringe (Becton, Dickson and Company, USA) every two weeks. 20 µl of the blood sample was suspended in 1 ml of RPMI Medium 1640 (Gibco, Thermo Fisher Scientific Inc. USA) for flow cytometry analysis and the rest of the blood was stored in Heparin microtubes (Sarstedt AG & Co, Germany) for lysozyme activity analysis. To measure growth, specific growth rate was calculated with $\frac{(\ln Weight_{Final} - \ln Weight_{Initial}) \times 100}{days}$. Final condition factors were calculated from the equation of Arfsten et al. (2010) for flatfish $\frac{weight \times 100}{(length \times width)^{3/2}}$ and Fulton's condition factor $\frac{weight \times 100}{length^3}$.

At the end of both short and long term experiments, all turbot were anaesthetized and blood and organ samples (gills, spleen, gut, liver, kidney, head kidney, and skin) were collected. Blood samples were used in flow cytometry and lysozyme activity analysis, and organ samples were stored in RNA stabilization reagent

(RNAlater) at -80 °C for molecular genetic analysis. Hepatosomatic index (HSI) of the long term study fish was calculated with $(\text{liver weight}/\text{fish weight}) \times 100$ and spleen-somatic index (SSI) was calculated with $(\text{spleen weight}/\text{fish weight}) \times 100$.

The tubercles of fish from the long term experiment were removed from the skin along the lateral line, rinsed with clean water, left to air dry over night, and stored for nanoindentation analysis.

2.5 FLOW CYTOMETRY

Live cells in turbot blood were analyzed with flow cytometry, a method where cells are identified and counted by size and morphology using their specific light characteristics. Fresh blood samples suspended in RPMI media (Gibco, Thermo Fisher Scientific Inc. USA) were washed twice with 1 ml RPMI by centrifuging with 6000 g for 10 min at 4 °C and discarding the supernatant. The samples were re-suspended in 450 µl RPMI and used for cell count analysis.

For the analysis, 150 µl of the samples were mixed with 100 µl of 20 µg/ml propidium iodide (Carl Roth GmbH, Germany) and 150 µl RPMI, and analyzed with a BD Accuri C6 Flow Cytometer set for a limit of 10,000 events in 'cells'. The amount of monocytes and lymphocytes measured in percentage were then calculated into proportions relative to all live cells measured from the sample, following Landis et al., 2012.

2.6 LYSOZYME ACTIVITY

The rest of the blood sample was centrifuged with 1400 g for 5 min at room temperature, the serum or supernatant was collected in microcentrifuge tubes and stored at -20°C for lysozyme activity analysis using the Sigma-Aldrich Lysozyme Activity Kit according to the manufacturer's protocol. 0.01% (w/v) stock *Micrococcus* bacteria solution was prepared before each week's measurements by dissolving *Micrococcus lysodeikticus* in the reaction buffer until the absorbance (450 nm) was 0.6-0.7 compared to a buffer blank. 25 µl of serum from each sample was mixed with 175 µl stock bacteria solution and immediately measured in a Tecan Infinite M200 spectrophotometer at 450 nm absorbance for a duration of 30 min in 30 sec intervals.

After measurements, the lysozyme concentration was calculated by the following equation: Units/ml enzyme = $\frac{(\Delta A_{450}^{Test}/\text{min} - \Delta A_{450}^{Blank}/\text{min})(df)}{(0.001)(\text{volume ml})}$ Where df = dilution factor, 0.001 = ΔA_{450} as per the Unit Definition (one unit lysozyme produces ΔA_{450} of 0.001 per minute at pH 6.24 and 25°C using *Micrococcus lysodeikticus* suspension as substrate in 2.6 ml reaction mixture), and volume = 0.1 (enzyme solution volume in ml).

2.7 MOLECULAR GENETIC ANALYSIS

2.7.1 RNA Extraction & cDNA Synthesis

Gills, spleen, head kidney, and skin samples from both long term and short term experiments were thawed over ice. Approximately 20 mg of these organ samples were used for RNA extraction with Stratec InviTrap Spin Universal RNA Kit. RNA extraction was conducted according to the manufacturer's protocol. Samples were placed in 900 μl Lysis Solution TR adjusted with 1/100 volume of β -Mercaptoethanol and homogenized with Zirconia beads from the kit (4 beads \times 0.7mm & 2 beads \times 1.2mm) using a TissueLyser II (QIAGEN GmbH, Germany) for 5 min at 25 Hz. The samples were then centrifuged and the supernatant was transferred into a new tube and mixed with 500 μl of molecular grade ethanol. The solution was pipetted onto the spin column and further washing steps followed the manufacturer's instruction with 30 μl of *Elution Buffer R used at the end for elution*. RNA concentration was measured with Nanodrop ND-1000 (Peqlab, Germany) and all samples were diluted to 100 ng/ μl with RNase-Free water. RNA samples were stored at -80°C.

Genomic DNA in RNA samples was removed using Quanta PerfeCta DNase I Kit (Quanta BioSciences, Inc. USA). For each sample, 8.5 μl (i.e. 850 ng) of RNA template were mixed with 1 μl 10x Reaction Buffer and 0.5 μl PerfeCta DNase I for a total reaction volume of 10 μl . The reaction mix was incubated using a thermocycler (PTC-200 Peltier Thermal Cycler, Bio-Rad Laboratories, Inc. USA) for 30 min at 37°C, 1 μl of 10x Stop Buffer was then added into each mix and incubated for 10 min at 65°C. The final product was then used for cDNA synthesis.

cDNA was synthesized using Quanta qScript cDNA Synthesis Kit (Quanta BioSciences, Inc. USA). For each sample, 7.5 µl of RNA was mixed with 2 µl of qScript Reaction Mix (5x) and 0.5 µl of qScript RT for a final volume of 10 µl. The reaction mix was then run in the thermocycler (PTC-200 Peltier Thermal Cycler, Bio-Rad Laboratories, Inc. USA) for 5 min at 22°C, 30 min at 42°C, and 5 min at 85°C. The final cDNA product was stored at -20 °C until further use.

2.7.2 Primers

A total of 32 target genes were analyzed for gene expression including genes for housekeeping, stress, apoptosis, glycolysis, immune response, antioxidant, and osmoregulation. 30 primers were designed by Joanna Miest (Miest & Bray, in prep; Miest et al., 2016) and 2 primers for osmoregulation, *Carbonic Anhydrase* and *V-type H⁺-ATPase*, were designed with BLAST search (NCBI) and Primer 3 Plus specifically for real-time PCR with a melting temperature of 60°C. Table 1 belows lists the complete list of primers used in this experiment.

Table 1: List of primers used in this experiment

Gene Type		Gene Name	Accession no.	Sequence	Name & Function
House Keeping		60S	DQ 848879.1	FW:GATGGTCCGCTACTCTCTCG RV:CACGGGTGTTCTTGAAGTGA	Ribosomal subunit 60S
		GAPDH	DQ 848904.1	FW:CAGTGTATGAAGCCAGCAGAG RV:ACCTGGATGTGAGAGGAG	Glyceraldehyde-3-Phosphate Dehydrogenase
		40S	DQ 848873.1	FW:GAAACAGCCCACCATCTTCC RV:GTAAGTGCCATCAATAGCCTCTC	Ribosomal subunit 40S
		Tubb	DQ 848894.1	FW:GAACACGGAATTGACCCAAC RV:GGGCACGTATTTACCACCTG	Tubulin β
Immune Response	Stress	HSP70	EF 191027.1	FW:CCGCTGCTGCTATTGCCTATGGT RV:TGCCGCCACCGAGATCAAAGATG	Heat shock protein 70 Stress protection
	Comple- ment	C3	DQ 400678.1	FW:TGACAATGGTGTGCTGTACT RV:CAATAGTCAAGGTCATTTGTGTTA	Complement component C3 Alternative pathway
		C1qB	DQ 848885.1	FW:CGGTGACCTACCAGAAGACC RV:GCGGAGTGGAAGGTGAAGTA	Complement Component 1, Q Subcomponent, B Chain
		CRP	JU 400100.1	FW:ACTACAAGCCGAACATGTGG RV:TGATGGTTGACCCAGAGATG	C-reactive protein
	Cytokine	IL1b	AJ 295836.2	FW:ACCAGACCTTCAGCATCCAGCGT RV:TTCAGTGCCCCATTCACCTTCCA	Interleukin β Pro-inflammatory cytokine
		TNFα	FJ 654645.1	FW:AAAAGAAGTCGGCTACGGGGTGGGA RV:TTCCAGTGCCAAGCAAAGAGCAGG	Tumor necrosis factor α Pro-inflammatory cytokine
		IFN1	KJ 150677.1	FW:GACGGGCATTATGGGTAGTG RV:CGTCTCTCCTCAGAGCCATC	Interferon 1 Antiviral, inflammation
		IFNγ	DQ 400686.1	FW:GCTTTCCCGATCATCTTCTG RV:GGTTTCCAGATTCCCATTC	Interferon-gamma
		Cytokine 17	HS 032344.1	FW:TTGTATTCTGGCCCTGCTG RV:TCAGCTCAGCATGAAAGGGG	Pro-inflammatory cytokine
		CXC	JF 913467.1	FW:ATCTTTCTGCTGGCTTGCAT RV:ATCTTTCTCGGTCGTGAGGA	Chemokine receptors

	Mucosal	Mucin18	JU 370277.1	FW:TTGTCCCTGACCAAGTGATG RV:ACAAAGCCTGTCCAAGATCG	Mucus forming
		Mucin2	JU 403288.1	FW:TGTTGGAGCAAGGAGAAACC RV:TTGTCTCAGGTTGGCAGTTG	Mucus forming
Adaptive Immune Response		CD45	FJ 226005.1	FW:GCGACTTCTGGTTGATGGTT RV:TGTCTGTGCTTGCAACTTCC	Cluster of differentiation 45
		CD8	JU 368863.1	FW:TTACATGGCTTCTGCTGCTG RV:AATGGCTGAAGTGCTTTGCT	Cluster of differentiation 8
		MHCII	HQ 698612.1	FW:AACAAGCTGGAGGTCACGAG RV:TTCCCACGTTGATGAGACA	Major histocompatibility complex class II
Innate Immune Response	Anti-microbial peptide	Hep1	AY 994075.1	FW:CTCCCTTTGCCGCTGGTG RV:AGCCCTTGTGGCCCTTGC	Hepcidin 1
		Hep2	JQ 219840.1	FW:ATGAAGACTCTCACCGTTGC RV:TTCTGTCTGTTACTCGGCATC	Hepcidin 2
		gLys	HQ 148717.1	FW:TCTCATTGCTGCCATCATCTC RV:CCACTCGGATTAACATCAACCT	g-type Lysozyme Bactericidal
		cLys	AB 355630.1	FW:GAACGCTGTGAATTGGCCGACT RV:GTTGGTGGCTCTGGTGTGTAGCTC	c-type Lysozyme Bactericidal
		beta-defensin1	JU 362659.1	FW:GGGAAAGGCTTCTTGTGTTG RV:TCTGTCTATCTCCTGTGATGC	Antimicrobial
		beta-defensin3	JU 352527.1	FW:GGAATGGCAAATGCTCAGAC RV:CATCGCTCAATGGTTTCTCC	Antimicrobial
		TLR3	FJ 009111.1	FW:GACGTGCTGATCCTGGTCTTCTGG RV:AGCTCAGGTAGGTCCGCTTGTTC	Toll like receptor 3 Pattern recognition receptor
		Trans	AJ 277079.1	FW:TTTGGCTTCCAGGATCTCCAG RV:CAGCTTTCGAGGAAGAAGTTGC	Transferrin Anti-bactericidal
Osmoregulation		CA	JU 378925.1	FW:ACTCCAATGGCATCCTCAAC RV:TGTTCCAGAAATGGGACCTC	Carbonic anhydrase Ion exchange
		HATPase	JU 389146.1	FW:TCACAGACGGAAGTGCTTC RV:TTCAGCCACACTTGGTATCG	V-type H ⁺ -ATPase Ion exchange
Antioxidant		SOD	HS 029499.1	FW:AAACAATCTGCCAAACCTCTG RV:CAGGAGAACAGTAAAGCATGG	Superoxide dismutase Antioxidant defense
Tight Junction		Cadherin	HS 032161.1	FW:ATGGGACACGCTATGACACA RV:ATCTCCATTTGCGTCGTGAT	Tight junction
Apoptosis		Caspase3	JU 391554.1	FW:TTCTGCCATTGTCTCTGTGC RV:GCCCTGCAACATAAAGCAAC	Pro-apoptotic
		Caspase7	JU 373310.1	FW:TCTGCAATGTCTCAACGAG RV:TTGCGACCATGTAGTTGACC	Pro-apoptotic
Glycolysis		G6P	KC 184131.1	FW:GGAAGCAAGAAATCCAGCAG RV:CGGCAACAATCATACCTGTG	Glucose-6-phosphate
		p450	JN 216889.1	FW:AGACGAGCAATGGAAGAGGA RV:GAAAGCAGTGCTGGTCACAA	Cytochrome p450 Metabolism

2.7.3 Gene Expression Analysis using qPCR (Gills)

Since only osmoregulation genes (2 genes) were analyzed in turbot gill samples, gene expression was measured with real-time quantitative PCR. The gill cDNA was diluted with water (PCR grade) at a 1:10 dilution before the analysis. The reaction mix composed of 2 µl 5x HOT FIREPol EvaGreen qPCR Mix Plus (Solis BioDyne, Estonia), 0.25 µl forward primer, 0.25 µl reverse primer, 5.5 µl PCR grade H₂O, and 2 µl of cDNA template. The qPCR was performed with the StepOnePlus Real-Time PCR System (Applied Biosystems/Thermo Fisher Scientific) with an incubation step at 95°C for 15

min, followed by 40 cycles of 95°C for 15 sec and 60°C for 1 min, and ending with a meltcurve: 95°C for 15 sec 60°C for 1 min, and an increase of 0.5°C/min until 95°C.

The gene expression (ΔCt) of each sample was calculated from the geometric mean of the housekeeping genes and used in statistical analysis. For illustration, gene expression relative to control was calculated according to the $2^{-\Delta\Delta\text{Ct}}$ method (Livak & Schmittgen, 2001) where $\Delta\Delta\text{Ct}$ of samples was calculated in relation to the mean ΔCt of the control group.

2.7.4 Gene Expression Analysis using the Fluidigm Biomark system (Head Kidney, Spleen, Skin)

Gene expression of all 32 genes in spleen, head kidney, and skin, was analyzed with qPCR Biomark HD system (Fluidigm, USA) based on 96.96 dynamic arrays (Gene Expression chips). Before the chip analysis, a pre-amplification step was performed. Each pre-amplification reaction mix contained 2.5 μl TaqMan PreAmp Master Mix (Applied Biosystems), 0.5 μl STA Primer Mix (500 nM primer pool from all primers in low EDTA TE buffer), 0.75 μl H₂O, and 1.3 μl cDNA. Amplification was run for 10 min at 95°C, then 14 cycles of 15 sec at 95 °C and 4 min at 60 °C. The final product was diluted 1:10 with low EDTA TE buffer. For the chip run, each sample mix contained 3.5 μl 2x SSoFast EvaGreen Supermix with low Rox (BioRad), 0.35 μl 20x DNA Binding Dye Sample Loading Reagent (Fluidigm), and 3.2 μl pre-amplified diluted cDNA. Each primer mix contained 3.5 μl 2x Assay Loading Reagent (Fluidigm), 3.15 μl low EDTA TE Buffer, and 0.7 μl Primer PreMix (50 μM of each primer pair). The chip run then followed the Fluidigm 96/96 Gene Expression Protocol with 5 standards and a blank water sample.

The raw data was evaluated using Fluidigm Real-Time PCR Analysis software and extracted for further analysis. Primer efficiency of all primers was verified to be similar. The stability of housekeeping genes was calculated with qBase+ software and the 3 most stable genes were used as reference genes by using the geometric mean for further calculations. Gene expression (ΔCt) of each sample was then calculated in relation to the reference genes and used for statistical analysis. Gene expression relative to control was calculated for illustration according to the $2^{-\Delta\Delta\text{Ct}}$ method (Livak & Schmittgen, 2001).

2.8 TURBOT SCALE MECHANICAL PROPERTY ANALYSIS

Only fish from control and highest CO₂ treatment in the long term experiment were used for analysis. Single tubercles were removed from along the upper lateral line of previously frozen defrosted fish and left to dry overnight. The point of interest in this experiment was the growth region which was along the edge of the tubercle. The edge of the dried tubercles was then cut off and fixed on a sample holder with liquid plastic welder (Bondic, Laser Bonding Tech, Inc., Aurora, Canada) (Fig. 4).

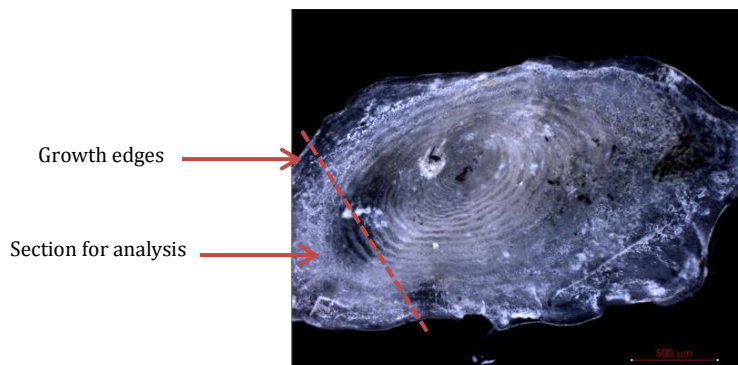


Figure 4: Example of a tubercle and the removed section (lower left corner)

To measure the mechanical properties, nano-sized indents were made on the edge of the tubercles using Nano Indenter SA2 (MTS Nano Instruments, Oak Ridge, TN, USA). The measurements were conducted at room temperature (22-25°C) with relative humidity 40-45%. The Continuous Stiffness Measurement (CSM) method was used to measure the changes in mechanical properties (Enders et al., 2004) with a maximum penetration depth of 500 nm at a constant strain of 0.05 s⁻¹.

The hardness and Young's modulus data for each sample, which provides information for the hardness and elasticity, respectively, were determined by processing load-displacement curves following methods by Oliver and Pharr (1992;2004). Data acquired from the machine was transferred into excel for graph plotting where both hardness and Young's modulus values at each depth were averaged for every 10 nm. The value at the plateau section of the graph was used as the final value of hardness and Young's modulus of each sample.

2.9 STATISTICAL ANALYSIS

All statistical analysis was performed with statistical software JMP 11.2 (SAS Institute Inc. 2013). All data was checked for normality and homogeneity of variances using Shapiro-Wilk test and Levene's test, respectively. Non normal data were transformed using log base 2. MANOVA was performed on gene expression data divided into functional gene groups. A two-way nested ANOVA was performed to analyze the effect of tank, time, treatment, and time-treatment interaction. A one-way ANOVA was performed to further investigate the effect between treatments within each time point. If there was a significance, a post hoc Tukey HSD test was used to determine the exact difference. For data that was not normally distributed after transformation, a Kruskal-Wallis test was performed instead of a normal one-way ANOVA.

3. RESULTS

3.1 WATER PROPERTIES

Water temperature increased throughout the course of the experiment from 10.8°C (lowest measurement) to 19.9°C (highest measurement) but was not different between treatments (Fig. 5). Except for pH, which was modified to mimic two different levels of ocean acidification, all other factors were kept constant throughout the experiment.

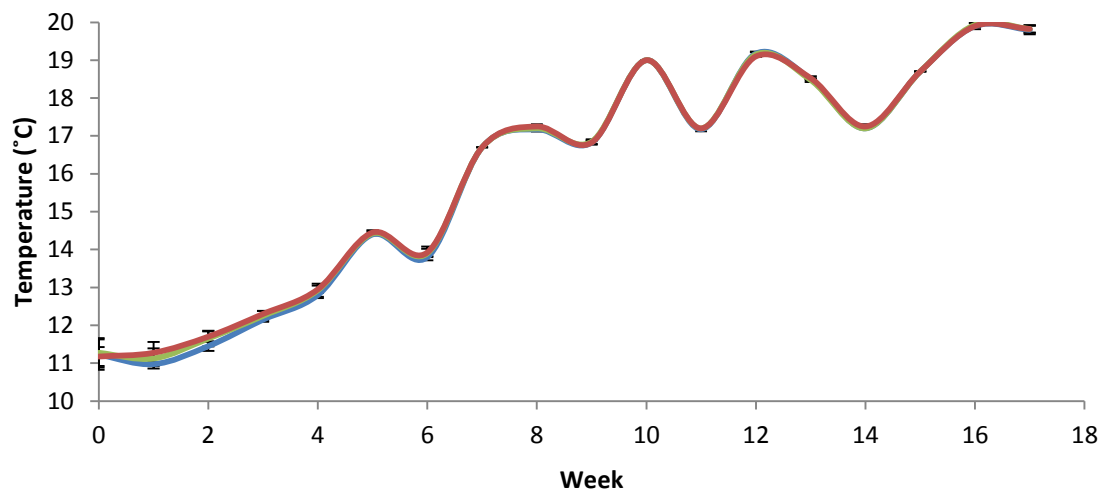


Figure 5: Mean daily water temperature (\pm SEM) of all treatments (calculated from 4 replicates for each treatment) throughout the experiment (blue line = ambient conditions, green line = medium pCO₂ ~1000 μatm, red line = high pCO₂ ~2000 μatm)

The pH in the control tanks fluctuated with the pH of the Kiel Fjord between 7.88-8.20. The pH in the medium CO₂ treatment varied from 7.76-7.87 and in the high CO₂ treatment from 7.45- 7.59 with no overlap between treatments (Fig. 6).

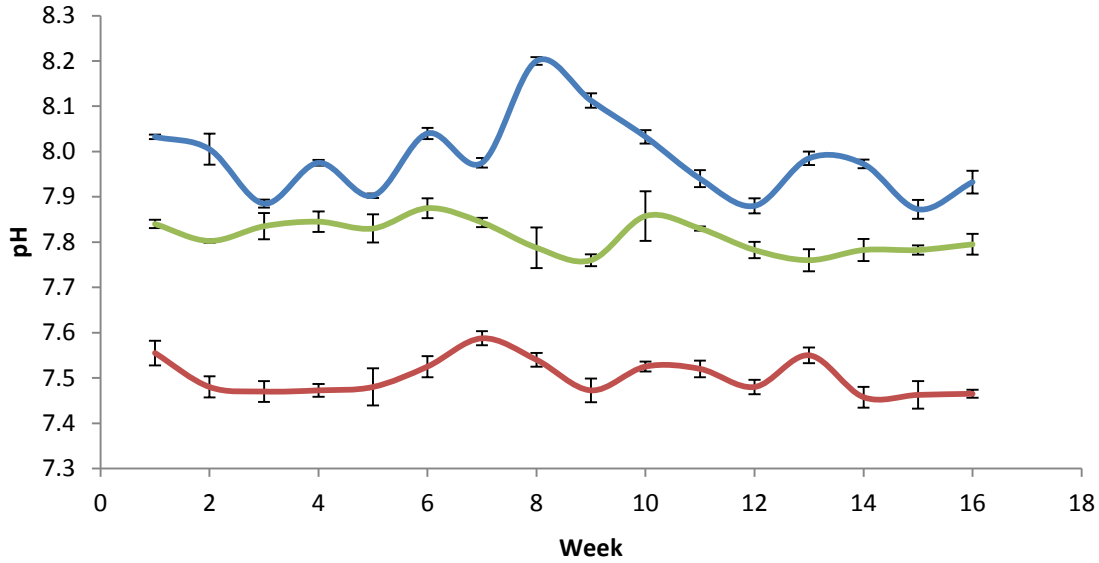


Figure 6: Average daily pH (\pm SEM) of all treatments throughout experiment (blue line = ambient conditions, green line = medium pCO₂ ~1000 μ atm, red line = high pCO₂ ~2000 μ atm)

pCO₂ was calculated from measured DIC and pH using CO2SYS (Lewis and Wallace, 1998) and the values for 1 week and 16 week experiment are displayed in Table 2 and 3 respectively.

Table 2: Carbonate chemistry values (\pm SEM) of 1 week experiment measured at start of experiment from all replicates tanks

Treatment	pH (NBS)	Alkalinity (μ mol/kgSW)	DIC (μ mol/kgSW)	pCO ₂ (μ atm)
Control	8.10	2080.38 \pm 3.93	2014.90	541.56
Medium CO ₂	7.77	2079.37 \pm 3.15	2115.75	1218.90
High CO ₂	7.55	2082.22 \pm 3.96	2124.52	2006.83

Table 3: Carbonate chemistry values (\pm SEM) of 16 week experiment measured at start of experiment and every 4 weeks after from all replicates tanks

Treatment	pH (NBS)	Alkalinity (μ mol/kgSW)	DIC (μ mol/kgSW)	pCO ₂ (μ atm)
Control	7.98 \pm 0.02	2008.23 \pm 13.10	1994.97 \pm 8.48	722.33 \pm 38.67
Medium CO ₂	7.80 \pm 0.01	2009.88 \pm 13.77	2045.33 \pm 6.16	1209.42 \pm 37.38
High CO ₂	7.50 \pm 0.01	2011.31 \pm 13.30	2117.86 \pm 6.78	2325.09 \pm 64.22

3.2 GROWTH & CONDITION

1 Week

Turbot in the 1 week experiment had an average starting weight of 170.8 ± 5.2 g and end weight of 176.9 ± 5.3 g. Average weight and specific growth rate of each treatment can be found in table 4 below.

Table 4: Average turbot weight \pm SEM and average specific growth rate \pm SEM in short term experiment

Treatment	Weight at Start (g)	Weight at End (g)	SGR (% BW/day)
Control	177.67 ± 7.75	178.50 ± 7.94	0.05 ± 0.43
Medium CO ₂	170.50 ± 10.24	170.50 ± 10.24	0.65 ± 0.8
High CO ₂	166.91 ± 9.52	171.27 ± 9.43	0.30 ± 1.0

There was no significant difference between the specific growth rates between treatments in the 1 week experiment ($df = 2$, $F = 0.2374$, $p = 0.7901$) as seen from the boxplots in Fig. 7.

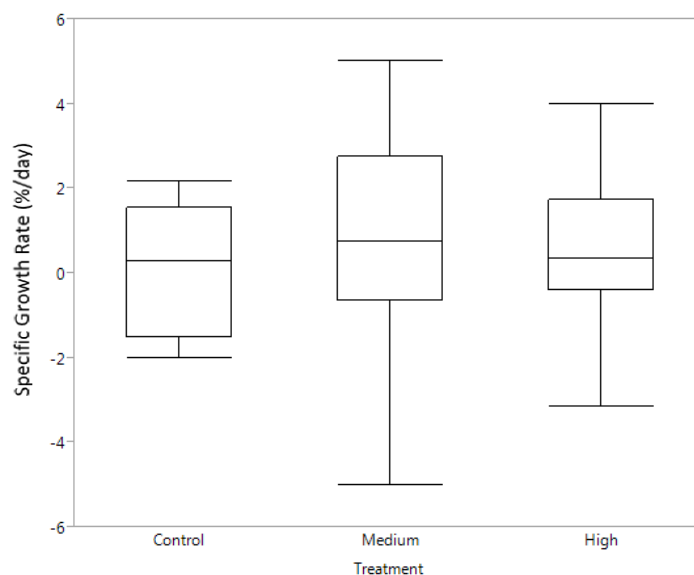


Figure 7: Specific growth rate (% Body Weight/day) between treatments of turbot from 1 week experiment. Box plot shows median, upper and lower quartile, minimum and maximum.

16 Weeks

The fish in the 16 week experiments had an average weight of 126 ± 3.3 g at the start of the experiment. No significant effect on final weight was detected between treatments (Control: 199 ± 8.54 g, medium: 208.17 ± 6.54 g, high: 199.33 ± 5.09 g). On average the turbot grew with a specific growth rate of 0.42 ± 0.02 % body weight gain/day and no significant difference was detected (Fig. 8).

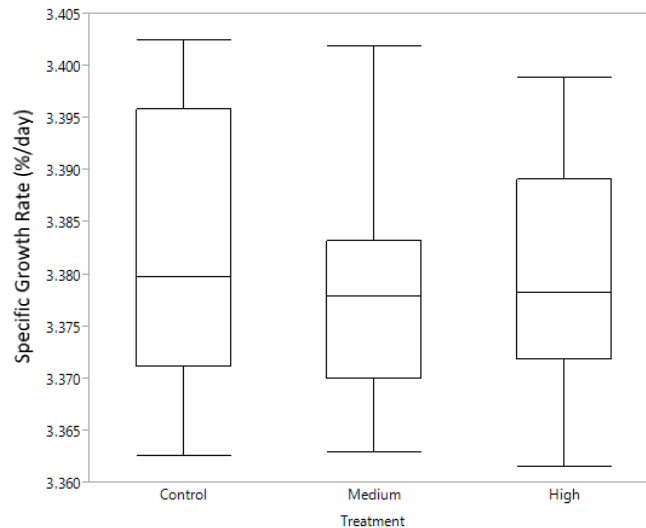


Figure 8: Specific growth rate (% BW/day) calculated from start to end between treatments of turbot from 16 week experiment. Box plot shows median, upper and lower quartile, minimum and maximum.

The bi-weekly specific growth rate did not differ between treatments in all time points (Fig. 9).

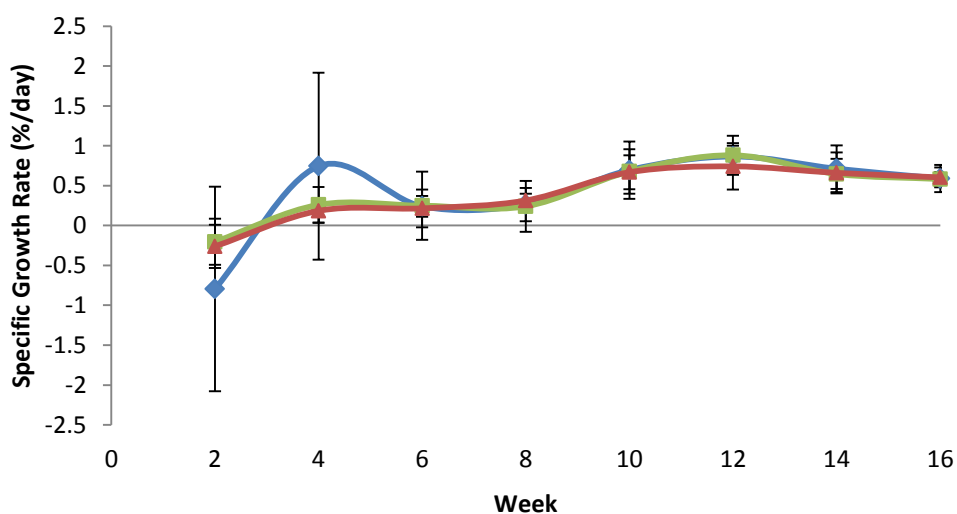


Figure 9: Specific growth rate (%/day) measured every 2 weeks of turbot from 16 week experiment (blue line = ambient conditions, green line = medium pCO₂ ~1000 µatm, red line = high pCO₂ ~2000 µatm)

Similarly to the specific growth rates, no difference was seen in the calculated condition factors (table 5).

Table 5: Condition factors of turbot between treatments in 16 week experiment. HSI = hepatosomatic index (calculated from liver weight to body weight ratio), SSI = spleen-somatic index, (calculated from spleen weight to body weight ratio), K = condition factor (calculated from body weight and length)

Treatment	HSI		SSI		K*		K**	
	Mean	SEM	Mean	SEM	Mean	SEM	Mean	SEM
Control	0.90	0.03	0.04	0.004	2.44	0.04	1.78	0.04
Medium CO ₂	0.90	0.04	0.05	0.003	2.44	0.03	1.75	0.02
High CO ₂	0.90	0.04	0.05	0.005	2.46	0.03	1.75	0.03

K* = The condition factor (CF) calculated using the weight and length data following the equation of Arfsten et al. (2010) for flatfish, $CF = (\text{weight} \times 100) / (\text{length} \times \text{width})^{3/2}$

K** = Fulton's condition factor = $\text{weight} \times 100 / \text{length}^3$ (Froese, 2006)

3.3 LYSOZYME ACTIVITY

1 week

After 1 week of CO₂ exposure (Fig. 10) lysozyme activity significantly increased (df = 2, F = 5.9590, p = 0.0062) in the highest CO₂ treatments (1790.76±153.39 units/ml enzyme) compared to the medium CO₂ (1298.78±89.75 units/ml enzyme, p = 0.0180) and the control treatment (1264.94±85.71 units/ml enzyme, p = 0.0113).

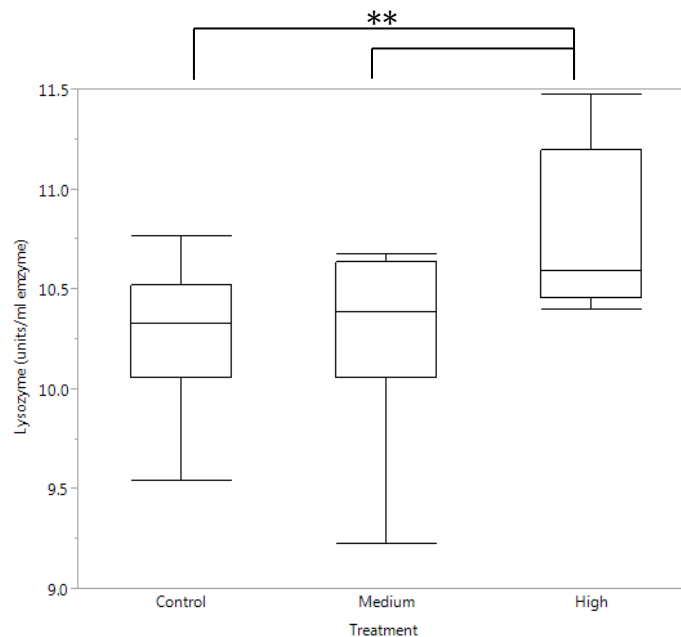


Figure 10: Lysozyme activity in turbot serum with confidence intervals in 1 week experiment (**p≤0.01). Box plot shows median, upper and lower quartile, minimum and maximum.

16 Week

In the long term experiment, most of the lysozyme activity did not differ across treatments. However when the p values of each time point are considered, a trend is indicated that the difference between treatments becomes greater over the weeks, especially lysozyme activity in week 6 (Control: 2151±123, medium: 1940±224, high: 1825±73 units/ml enzyme, $p = 0.0498$), until week 10 (lysozyme activity Control: 3043±111, medium: 2869±169, high: 2568±112, $p = 0.0518$) and then the difference gradually disappears until the end of the experiment (Fig. 11).

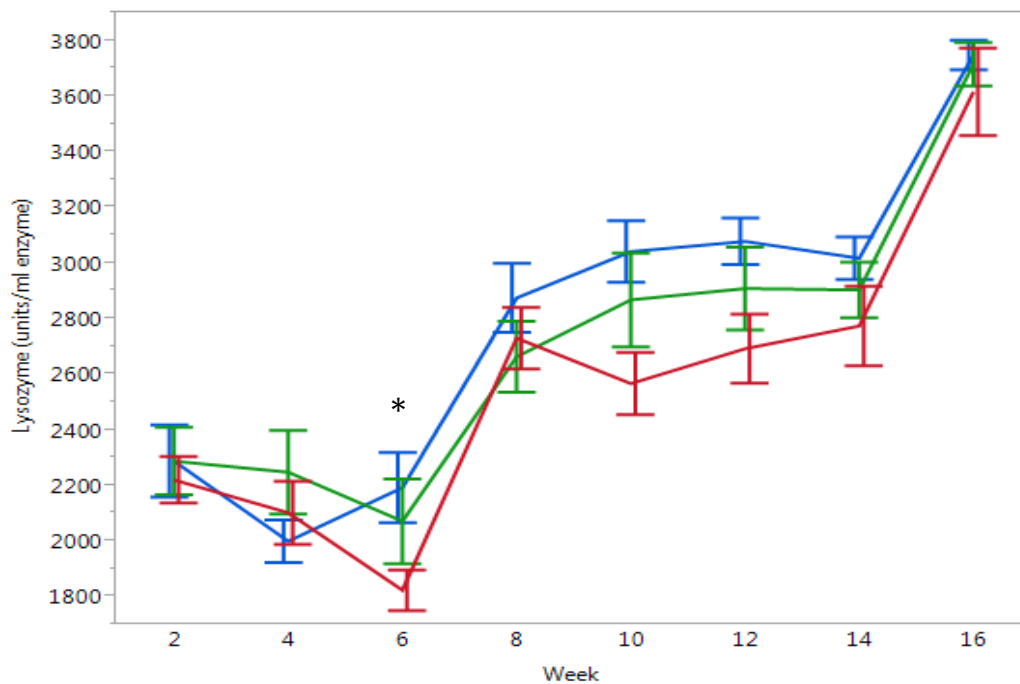


Figure 11: Mean lysozyme activity \pm SEM in turbot serum measured every 2 weeks in 16 week experiment (blue line = ambient conditions, green line = medium pCO₂ ~1000 μ atm, red line = high pCO₂ ~2000 μ atm) (* $p < 0.05$)

3.4 GENE EXPRESSION

Treatment Effect

Gills

Carbonic anhydrase (ca) expression in the gills was not significantly affected by the CO₂ exposure in both the short term (df = 2, F = 0.6274, p = 0.5444) and long term experiment (df = 2, F = 0.0092, p = 0.9908) as seen from Fig. 12.

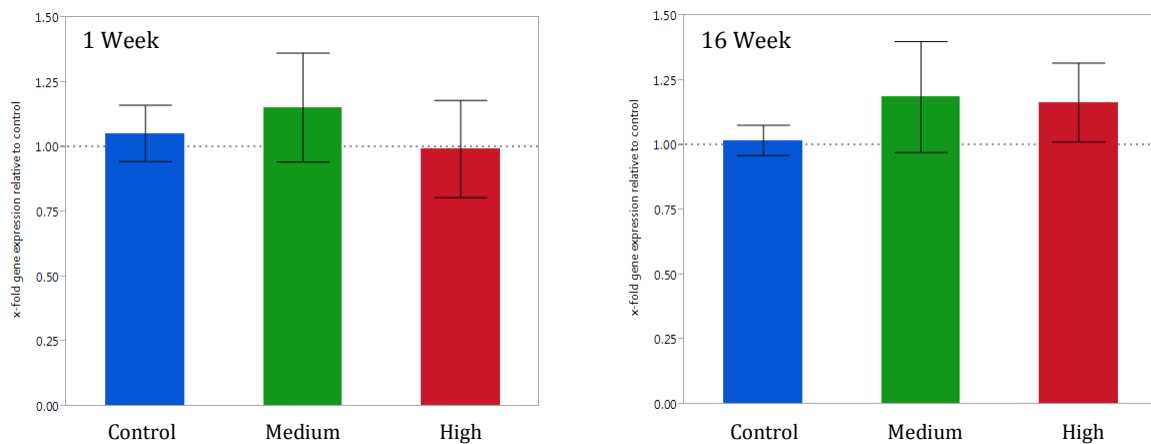


Figure 12: Mean *ca* gene expression (relative to control) \pm SEM in turbot gills compared between treatments from 1 week and 16 week experiments

V-type *H*⁺-*ATPase* average gene expression was not affected by the CO₂ exposure at any time point. However time significantly affected gene expression in the medium CO₂ treatment (t = 3.61, df = 22, p = 0.0016) (Fig. 13). In the short term study, *V*-type *H*⁺-*ATPase* gene expression of 1.02 \pm 0.07-fold (Δ ct = 6.99 \pm 0.09) was higher in this treatment than in the long term study of 0.69 \pm 0.06-fold (Δ ct = 7.61 \pm 0.15). Though statistically not significant (p=0.16), the Control group also displayed a trend of *H*⁺-*ATPase* down regulation in the long term experiment (1 week: 1.13 \pm 0.15-fold, Δ ct = 7.13 \pm 0.24, 16 week: 0.80 \pm 0.06-fold, Δ ct = 7.51 \pm 0.11). Statistical tests showed that *v*-type *H*⁺-*ATPase* gene expression in gills was not significantly influenced by the CO₂ treatments in both the 1 week (df = 2, F = 0.6730, p = 0.5177) and the 16 week experiment (df = 2, F = 1.5584, p = 0.2260).

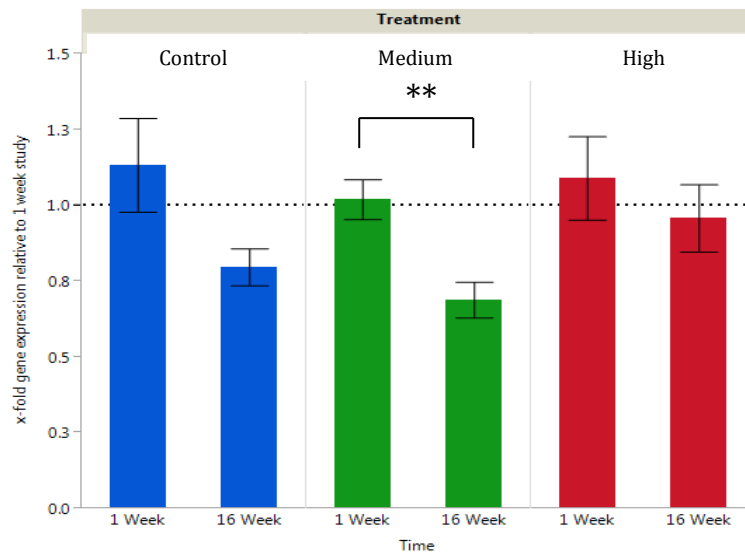


Figure 13: *V-type H⁺-ATPase* gene expression (relative to 1 week study) ± SEM in turbot gills compared between time from 1 week and 16 week experiments (**p≤0.01)

Head Kidney

Multivariate analysis of head kidney gene expression in short term study revealed that genes involved in immunity (*c3, il1b, tnfa, c1qb, cd8, cytokin 17, cxc, mhci, cd45, glyx, clys, tlr3, beta-defensin1&3, crp, ifn1, ifng, mucin2&18, hsp70*), osmoregulation (*ca* & *H⁺-ATPase*), antioxidant (*sod*), tight junction (*cadherin*), and glycolysis (*g6p* & *p450*) were not affected by elevated CO₂ levels. Antimicrobial genes however were significantly affected by CO₂ treatments (F=2.54, p=0.0304) as well as apoptosis genes (F=2.88, p=0.0301).

Upon further investigation into apoptosis genes, *caspase 3* was found to be significantly down regulated (df = 2, F = 6.6012, p = 0.0063) in the highest CO₂ treatment (0.80±0.05-fold, Δct = 5.13±0.08) compared to Control (1.02±0.06-fold, Δct = 4.79±0.09) in the short term experiment (Tukey HSD p = 0.0169) (Fig. 14).

Similarly at the same time point, gene expression of *hepcidin-1*, from antimicrobial gene group, in the high CO₂ treatment (0.59±0.08-fold, Δct = 7.07±0.19) was significantly down-regulated (df = 2, F = 5.1625, p = 0.0116) compared to Control (1.16±0.21-fold, Δct = 6.20±0.23, p = 0.0144) and medium CO₂ treatment (0.93±0.14-fold, Δct = 6.65±0.40, p = 0.0428) (Fig. 14).

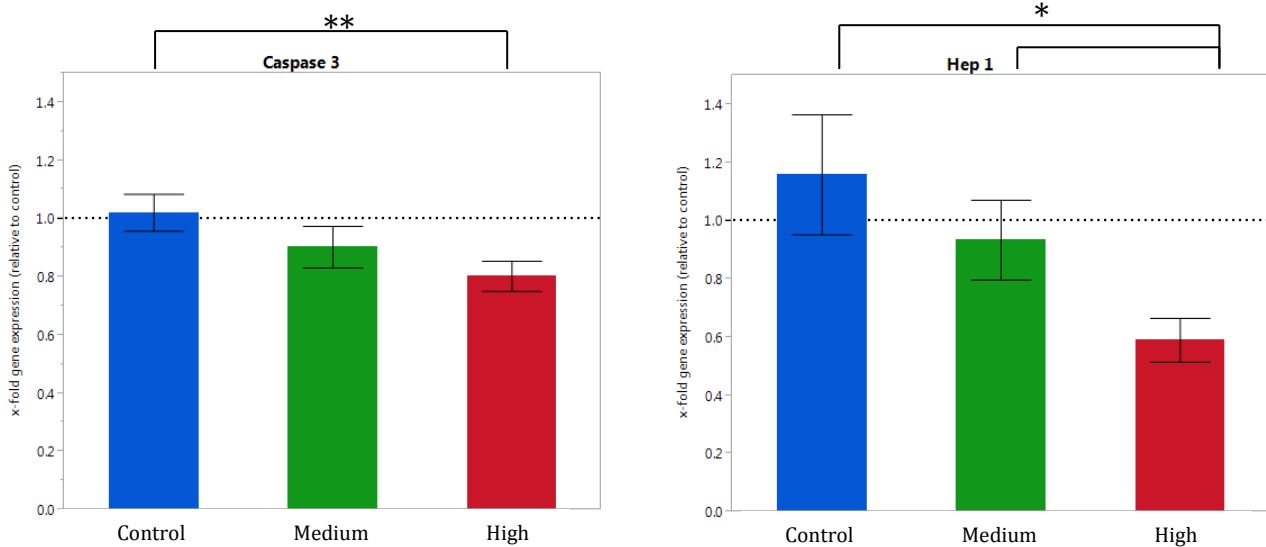


Figure 14: *Caspase-3* and *Hepcidin-1* (Hep1) gene expression (relative to control) ± SEM from turbot head kidney between treatments from 1 week experiment (* $p < 0.05$, ** $p \leq 0.01$)

Following a similar pattern found in the short term experiment, MANOVA revealed an effect of CO₂ on apoptosis genes ($F=2.52$, $p=0.0495$) in the long term study, which was expressed in the decrease of *caspase 7* expression ($df = 2$, $F = 6.4551$, $p = 0.0397$) of the high CO₂ treatment (0.71 ± 0.04 -fold, $\Delta ct = 6.47 \pm 0.08$) compared to the Control group (1.08 ± 0.14 -fold, $\Delta ct = 5.95 \pm 0.17$, Tukey HSD $p = 0.0455$) (Fig. 15).

Also in the long term study, mucus genes were found to be effected by treatment ($F=4.03$, $p=0.0060$). Further analysis revealed a down regulation of *mucin 2* ($df = 2$, $F = 3.9149$, $p = 0.0317$) in the medium CO₂ treatment (0.36 ± 0.09 -fold, $\Delta ct = 17.14 \pm 0.41$) compared to the high CO₂ treatment (3.85 ± 1.61 -fold, $\Delta ct = 14.33 \pm 0.66$, Tukey HSD $p = 0.0455$) (Fig. 15).

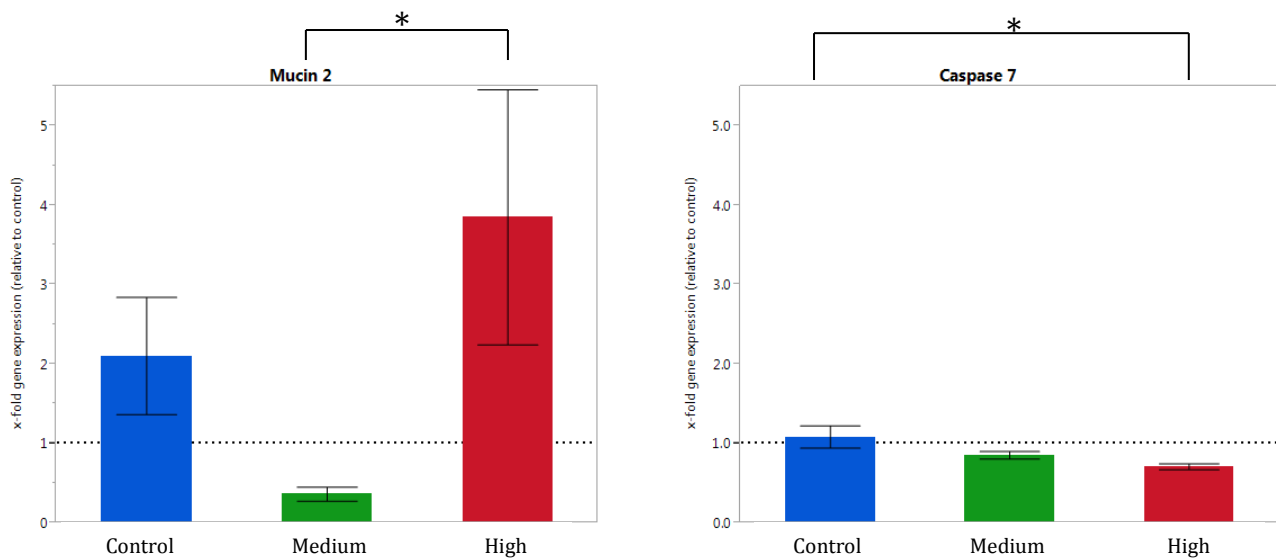


Figure 15: *Mucin-2* and *Caspase-7* gene expression (relative to control) \pm SEM from turbot head kidney between treatments from 16 week experiment (* $p < 0.05$)

Spleen

Multivariate analysis on spleen gene expression revealed that most genes were not affected by an increase in CO_2 in the short term study, such as immunity genes, (*c3*, *il1b*, *tnfa*, *c1qb*, *cd8*, *cytokin 17*, *cxc*, *mhcii*, *cd45*, *hep2*, *glys*, *clys*, *tlr3*, *beta-defensin1&3*, *crp*, *ifn1*, *ifng*, *trans*, *mucin2&18*, *hsp70*), osmoregulation genes (*ca* & *H⁺-ATPase*), antioxidant gene (*sod*), tight junction gene (*cadherin*), glycolysis genes (*g6p* & *p450*), and apoptosis genes (*caspase3&7*).

As already seen in head kidney *hepcidin 1*, in the short term study, spleen *hepcidin 1* in high CO_2 (0.63 ± 0.10 -fold, $\Delta\text{ct} = 7.15 \pm 0.22$) was also down regulated ($\text{df} = 2$, $F = 3.5126$, $p = 0.0414$) compared to the Control (0.95 ± 0.13 -fold, $\Delta\text{ct} = 6.50 \pm 0.19$; Tukey HSD $p = 0.0347$) (Fig. 16).

Another gene affected by CO_2 was *sod*, which was up regulated ($\text{df} = 2$, $F = 9.0319$, $p = 0.0109$) in the short term study, with the medium CO_2 treatment gene expression (1.27 ± 0.08 -fold, $\Delta\text{ct} = 2.68 \pm 0.09$) higher than both the Control (1.01 ± 0.05 -fold, $\Delta\text{ct} = 2.99 \pm 0.07$, $p = 0.0226$) and the high CO_2 treatment (0.87 ± 0.07 -fold, $\Delta\text{ct} = 3.26 \pm 0.14$, $p = 0.0062$) (Fig. 16).

Interestingly, these effects disappeared during long term CO_2 exposure, when no differences in gene expression were detected in spleen.

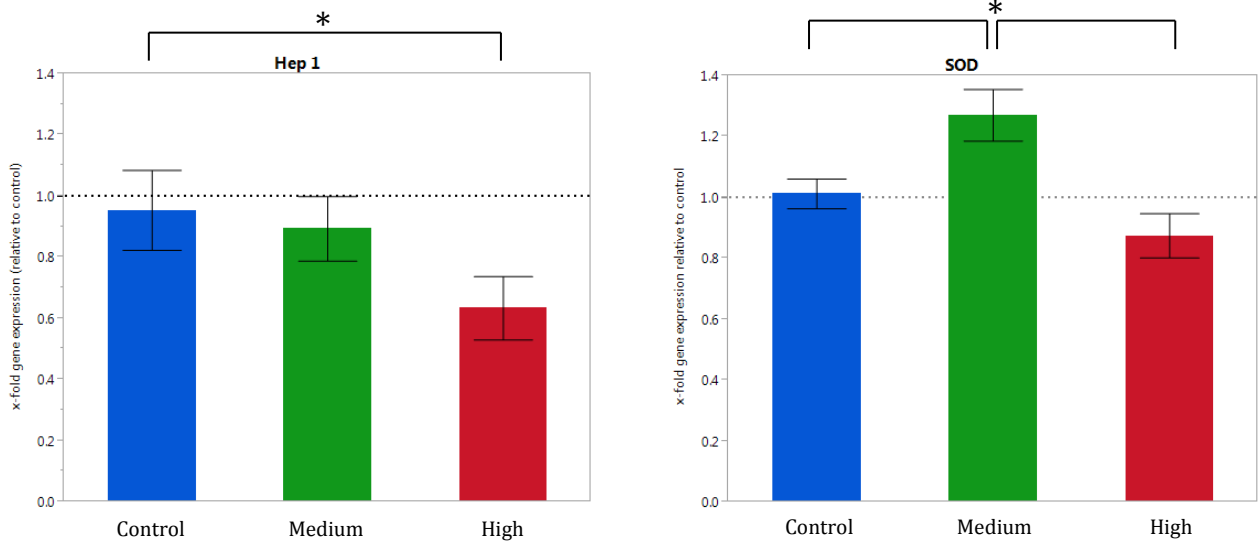


Figure 16: *Hepcidin-1* (Hep 1) and *sod* gene expression (relative to control) ± SEM from turbot spleen between treatments from 1 week experiment (* $p < 0.05$)

Skin

Gene expression in skin tissue was only analyzed for the ambient and high treatment. Only *cadherin* was found to be affected by elevated CO₂ levels. During the 1 week experiment, *cadherin* was up regulated ($t = -3.27$, $df = 16$, $p = 0.0048$) in the high CO₂ treatment (2.64±0.27-fold, $\Delta ct = 6.82 \pm 0.16$) compared to Control treatment (1.27±0.25-fold, $\Delta ct = 8.15 \pm 0.41$) (Fig. 17). No differences in gene expression were observed at 16 weeks.

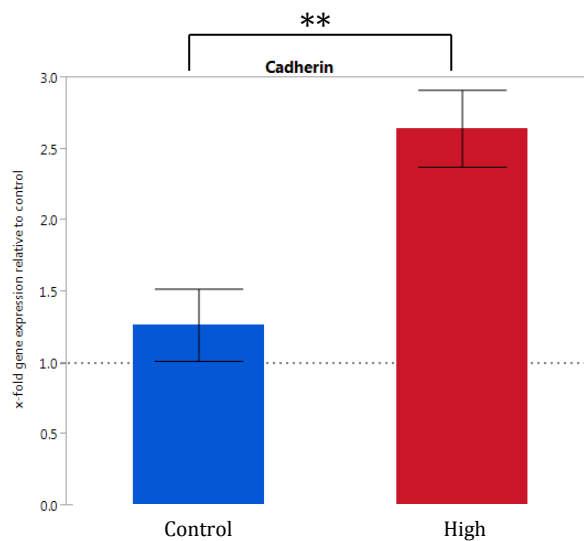


Figure 17: *Cadherin* gene expression (relative to control) ± SEM from turbot skin between treatments from 1 week experiment (** $p \leq 0.01$)

Time Effect

Although treatment did not affect mRNA levels of most genes, some of the studied genes were influenced by the duration of the treatment (Fig. 18). In turbot head kidney some genes (*c3*, *ca*, *caspase 3*, *gapdh*, *glys*, *sod*) were up-regulated in the long term exposure compared to the acute exposure independent of treatment (df =1, $F > 9$, $p < 0.003$) (Fig. 18A). As for the spleen, both up- and down-regulated genes were found in the long term treatment (df=1, $F > 11$, $p < 0.0014$) which can be seen in Fig. 18B and 18C. All gene expressions were relative to the Control group of the 1 week experiment.

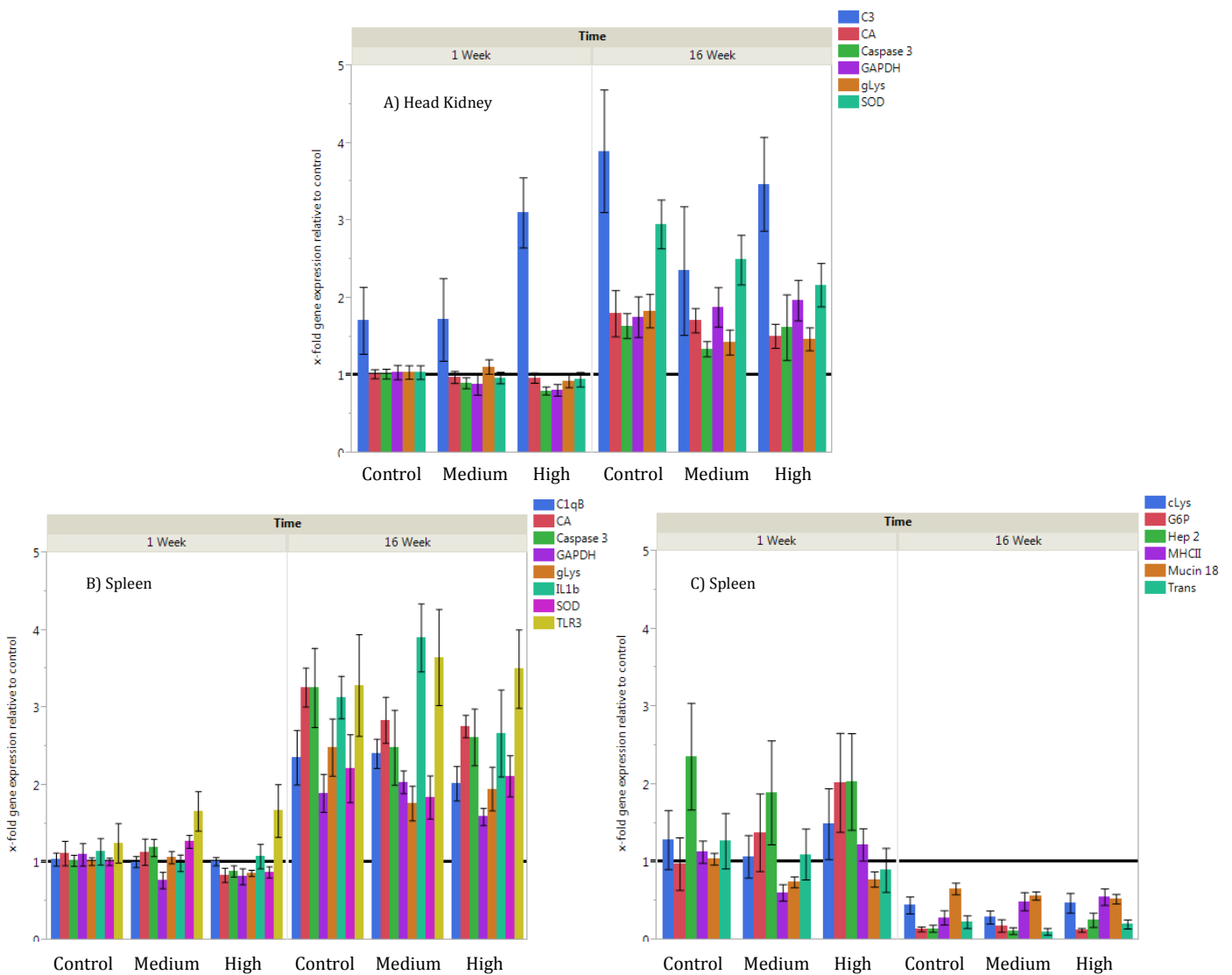


Figure 18: Mean gene expression relative to short term Control \pm SEM from 1 week and 16 week experiments in turbot head kidney (A) and spleen (B&C)

3.5 BLOOD COUNT

1 Week

The analysis of blood cell composition of fresh turbot blood from week 0 and week 1 of the short term experiment showed that at the start of the study (week 0), fish had a lymphocyte proportion on average (relative to all live cells) of 0.52 ± 0.03 and a monocyte average proportion of 0.56 ± 0.02 . No significant effect of final lymphocyte (Control: 0.57 ± 0.03 , medium: 0.60 ± 0.02 , high: 0.65 ± 0.01) and monocyte proportion (Control: 0.54 ± 0.03 , medium: 0.50 ± 0.02 , high: 0.46 ± 0.01) was detected between treatments or time (Fig. 19).

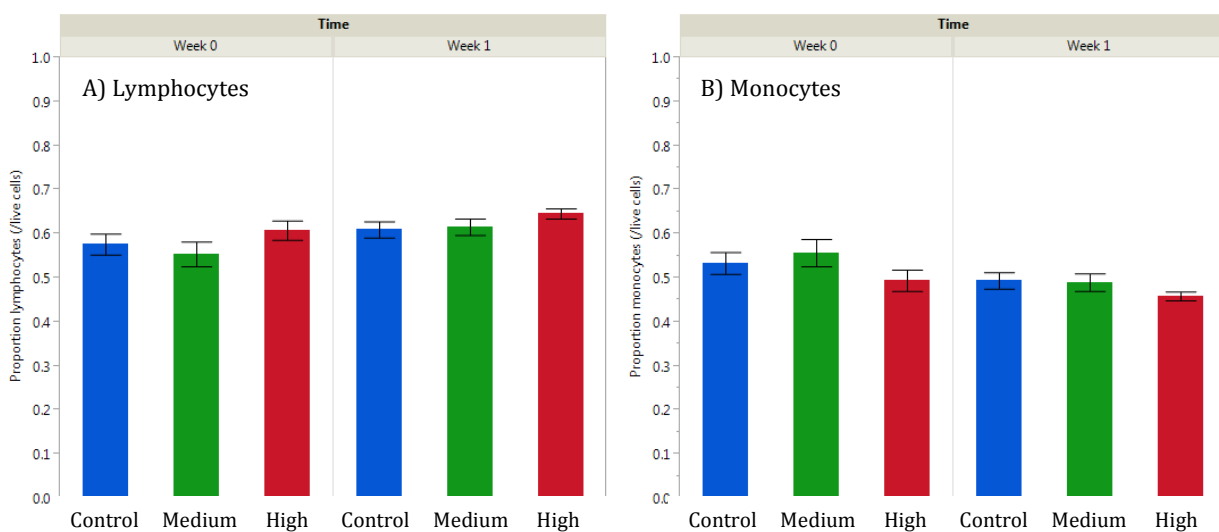


Figure 19: Mean proportion of lymphocytes (A) and monocytes (B) relative to all live cells \pm SEM in fresh turbot blood from 1 week experiment

16 Week

As for the long term study (Fig. 20), monocytes ($df=2$, $F=4.5844$, $p=0.0175$) and lymphocytes ($df=2$, $F=4.6742$, $p=0.0163$) at almost all time points were not affected by CO_2 , except for week 16. In the last week of the long term study, average proportion of lymphocytes in the medium treatment (0.74 ± 0.02) was significantly higher (Tukey HSD $p=0.0215$) than the Control (0.66 ± 0.02). Monocytes displayed an opposite trend, with average proportion monocytes in medium CO_2 treatment (0.37 ± 0.02) significantly lower (Tukey HSD $p=0.0260$) than the Control (0.45 ± 0.02).

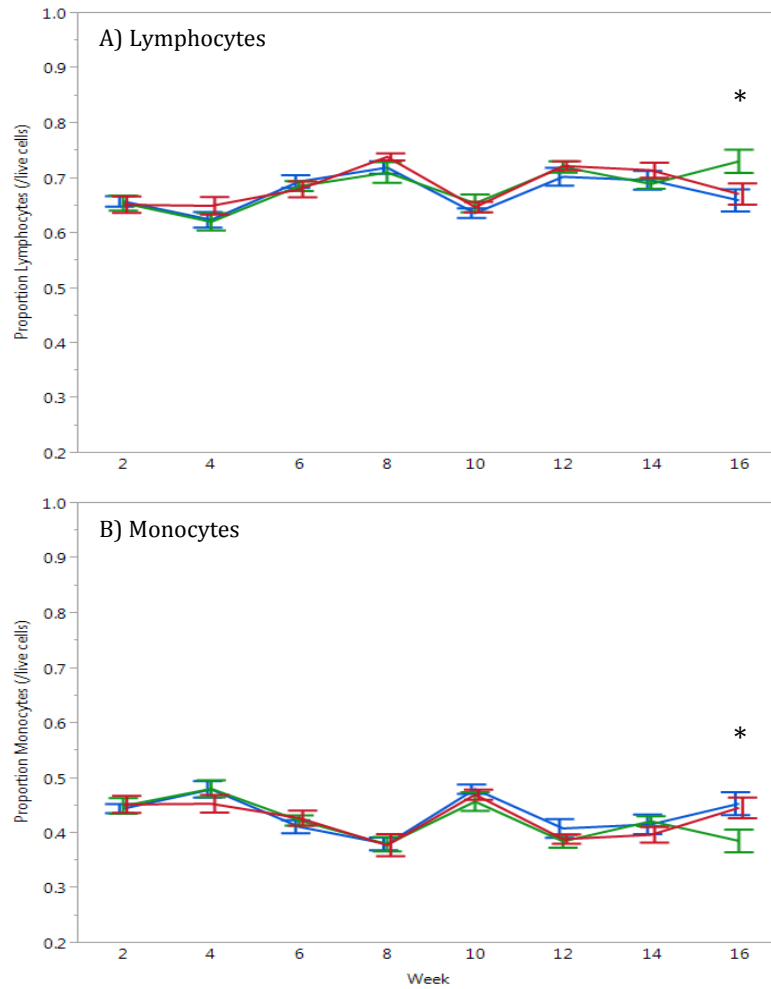


Figure 20: Bi-weekly mean proportion of lymphocytes (A) and monocytes (B) relative to all live cells \pm SEM in fresh turbot blood from 16 week experiment (blue line = ambient conditions, green line = medium pCO₂ \sim 1000 μ atm, red line = high pCO₂ \sim 2000 μ atm) (*p<0.05)

3.6 SCALE MECHANICAL PROPERTIES

Images of turbot scales, also referred to as tubercles, were obtained with a stereo light microscope Leica M205A (Leica, Wetzlar, Germany) at 20 X and 50 X magnification (Fig. 21). Images reveal that most of the tubercle, including the growth region of interest, lies under the skin (Fig. 21A & 21B). Shape and size of the whole tubercle can be seen after removal from the skin in Fig. 21C & 21D.

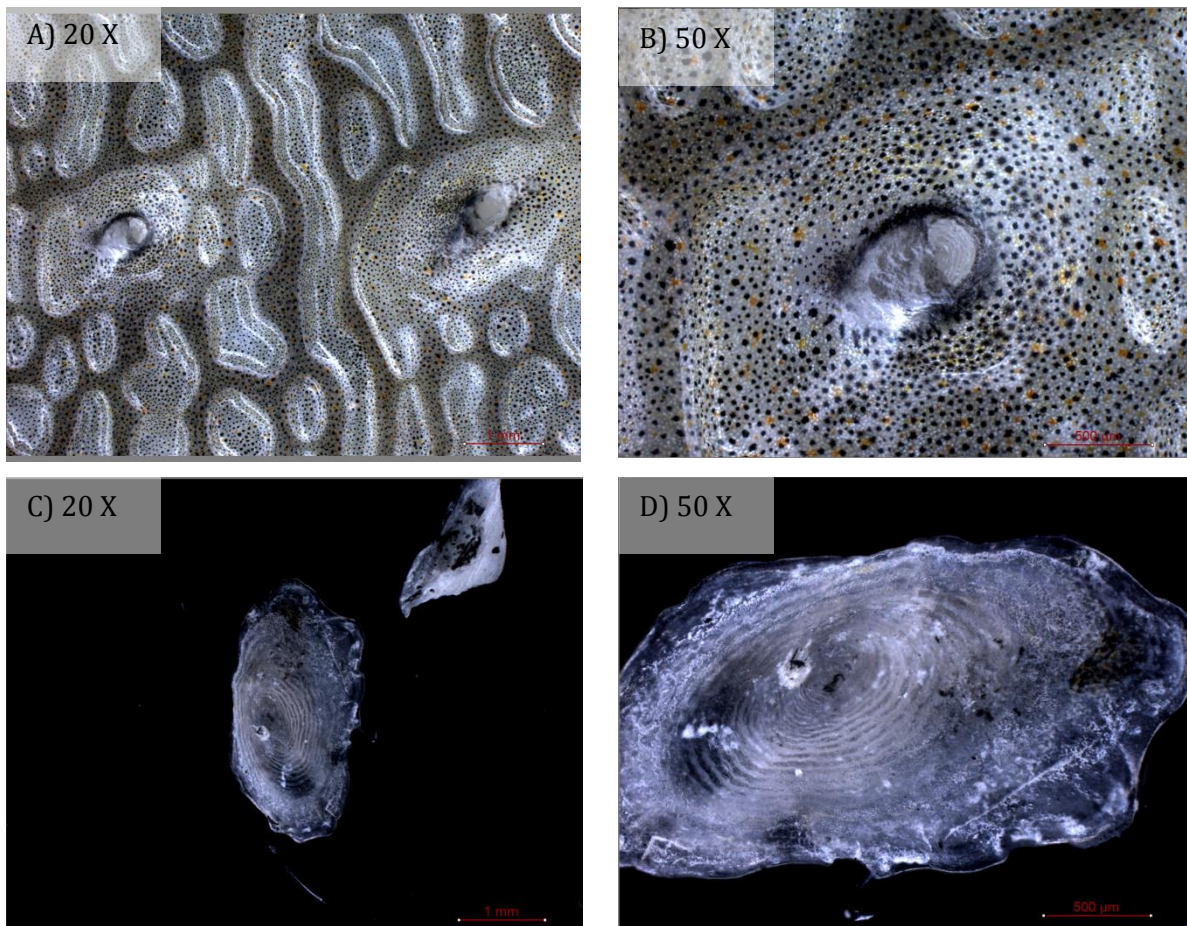


Figure 21: Stereo light microscopy images of turbot tubercle at 20X and 50X magnification captured before removal (A&B) and after removal from skin (C&D)

Turbot scale properties were only analyzed in the ambient and high CO₂ conditions of the long term experiment. Measurements from 200nm-500nm into the surface contained the most constant values; therefore the average measurement values from this region were used for comparison of elastic modulus and hardness between treatments.

Young's Modulus

In the 16 week experiment, tubercle analysis determined the average Young's modulus, or elastic modulus, between 200-500 nm depth of the Control group to be 5.31 ± 0.13 GPa and the high CO₂ group to be 4.78 ± 0.10 GPa (Fig. 22). A lower Young's modulus value represents a more flexible material, and similarly a high modulus value signifies a more stiff material. Statistical analysis revealed no significant effect of CO₂ on the Young's modulus of the turbot tubercle ($t = -1.66$, $df = 18$, $p = 0.1144$).

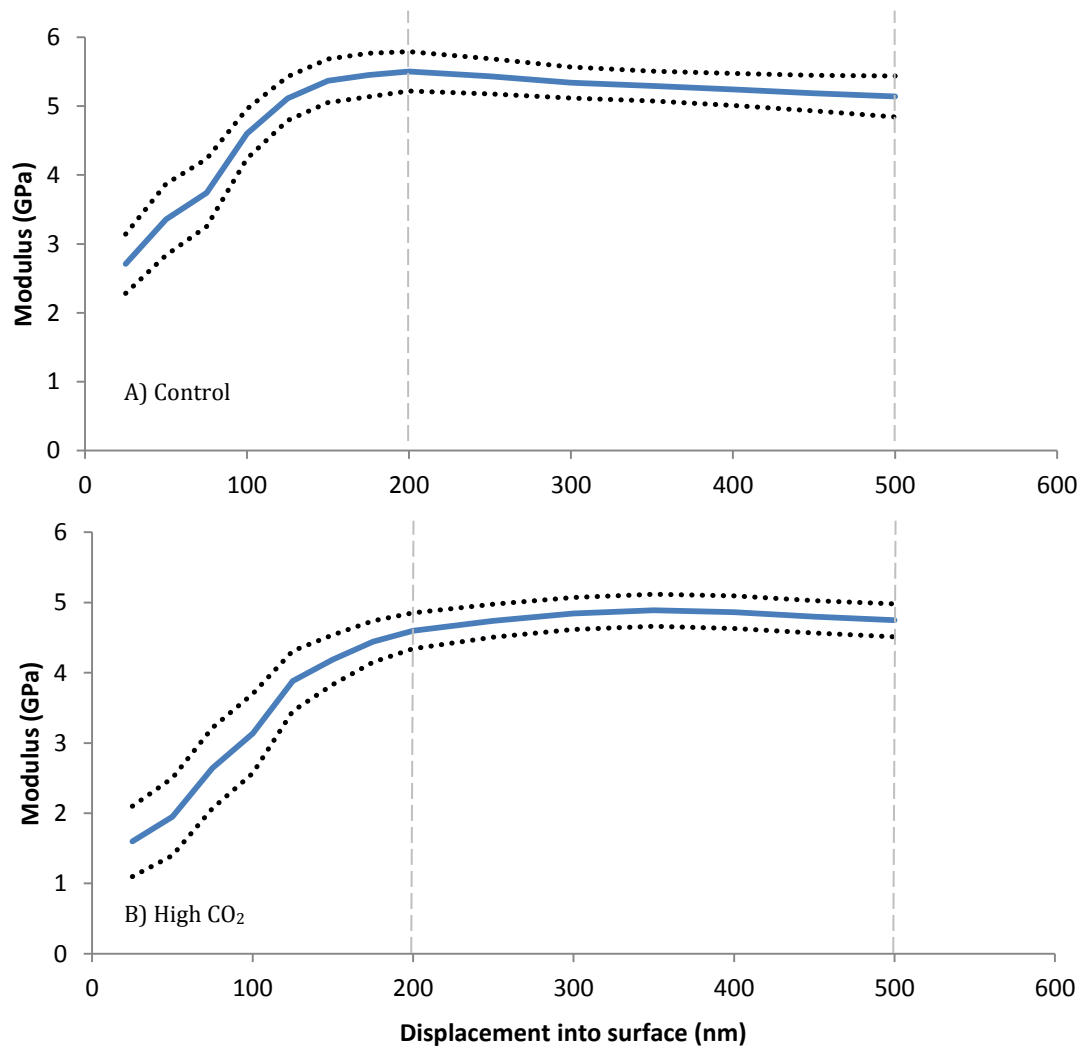


Figure 22: Average Young's Modulus of turbot tubercle from Control (A) and high CO₂ (B) treatment. Blue line represents average modulus, dotted lines represent the upper and lower standard error of mean (SEM)

Hardness

As for the hardness measurements, similar to the Young's modulus results, there was no significant difference of scale hardness ($t = 0.10$, $df = 18$, $p = 0.9192$) between turbots from the Control group (0.163 ± 0.011 GPa) and the high CO_2 treatment (0.165 ± 0.004 GPa) between 200-500 nm depth in the long term study (Fig. 23).

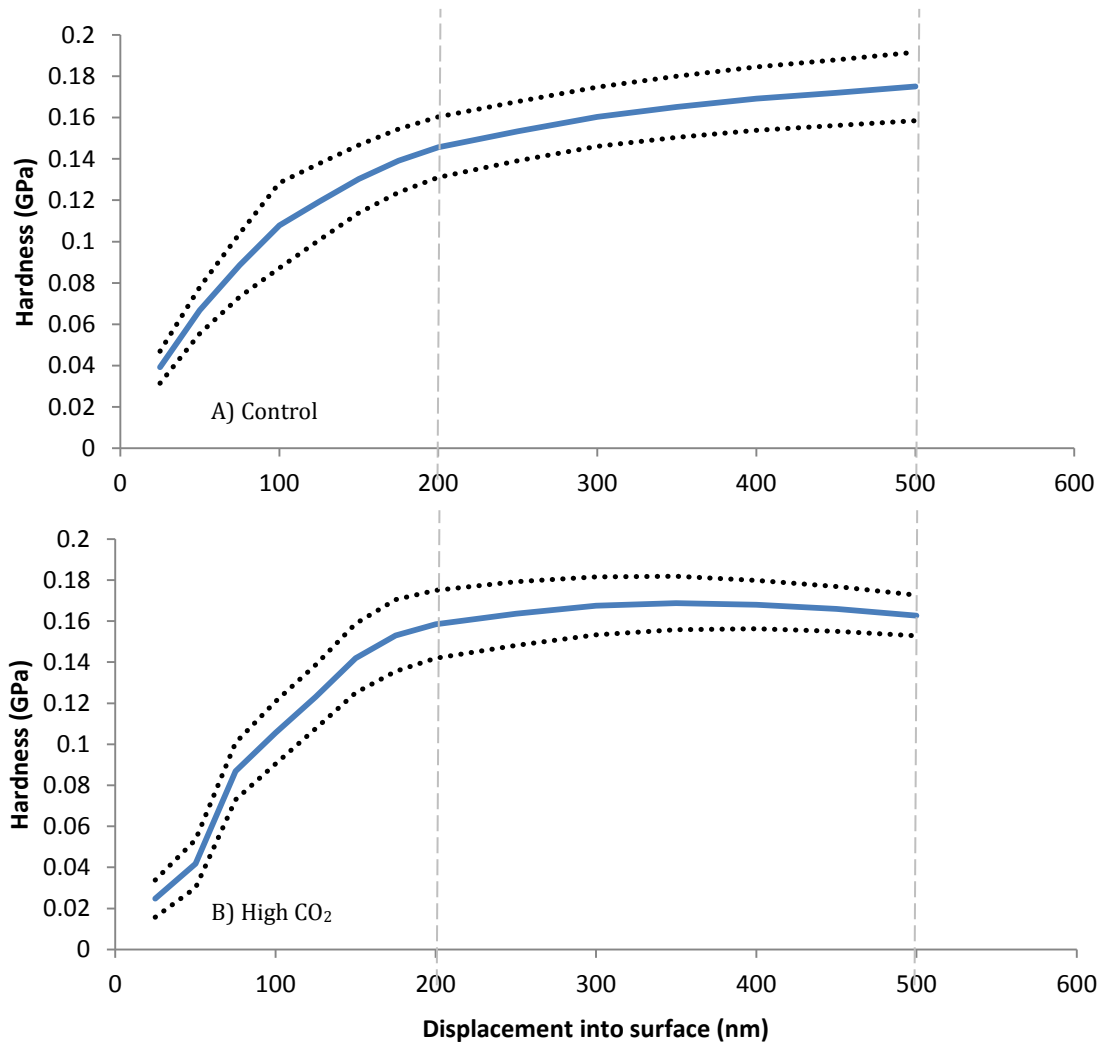


Figure 23: Average hardness of turbot tubercle from Control (A) and high CO_2 (B) treatment. Blue line represents average hardness, dotted lines represent the upper and lower standard error of mean (SEM)

4. DISCUSSION

This study was conducted to investigate the effect of elevated CO₂ on immune response and scale mechanical properties of juvenile turbot. Turbot is a commercially important fish in aquaculture (Froese & Pauly, 2015) and this study is beneficial for understanding the acclimation potential of turbot to increasing CO₂ levels. Knowledge of their response to future predicted levels of oceanic CO₂ is essential to predict the impacts of ocean acidification on fisheries and aquaculture production which in turn is relevant to climate change policies and management.

As suggested by Heuer & Grosell (2014) short term CO₂ exposure experiments have limited ability in assessing species' adaptive capacity, and juvenile turbot in a study by Stiller et al. (2015) were able to acclimatize to hypercapnic conditions after two weeks, the experiment in this study therefore consisted of two parts. A short term experiment to analyze acute effects on immunity and a long term experiment of 16 weeks, in order to investigate the acclimation ability of turbot's immune responses over time, was performed.

4.1 WATER PROPERTIES

Throughout both experiments all abiotic factors were kept similar between treatments. pH levels were experimentally manipulated and led to a difference in pCO₂ concentrations. Temperatures varied throughout the course of the experiment following the seasonal Kiel Fjord water temperature but were similar between treatments. Even though pH levels fluctuated, partially due to the fluctuation of pCO₂ in the Baltic Sea water (Melzner et al., 2013; Thomsen et al., 2013), mean pH values of each treatment did not overlap, suggesting CO₂ concentration to be the cause of treatment effects in this study. Carbonate chemistry revealed a relatively high CO₂ concentration in the control groups, which was due to the high CO₂ levels in seawater of the Kiel Fjord and Kiel Bay (Melzner et al., 2013) and were not removed in the experimental tanks.

4.2 GROWTH

Fish growth is an important bioindicator for fish habitat quality (Gilliers et al., 2006), water quality (Viadero, 2005; Budy et al., 2011), and environmental stress (Pankhurst & Van Der Kraak, 1997; Barton et al., 2002; Van Weerd & Komen, 1998). Understanding and determining environmental factors that can impact fish growth is crucial to aquaculture production and fisheries management.

The specific growth rate of turbot in both the short and long term experiment did not indicate a treatment effect or time effect from elevated CO₂. Similarly, in the long term experiment, the bi-weekly specific growth rate was not significantly different between each measurement point and all fish in the experiment had similar final condition factor values. This is in contrast to a recent study by Stiller et al. (2015) where a decrease in specific growth rates of juvenile turbot exposed to elevated CO₂ was observed. However, this study was performed in a recirculating system where the authors used pCO₂ levels of 15,000 and 25,000 µatm, which is more than 7 times higher than the highest CO₂ concentration used in this experiment. Though Stiller et al. (2015) used a recirculating system, the fish were in a flow-through respirometer with constant CO₂ degassing (Stiller et al., 2015; 2013), and a similar method of CO₂ injection into the system was used. Perhaps not directly comparable, the study from Stiller et al. (2015) can still provide useful information on the effect of elevated CO₂ on juvenile turbot growth. Therefore, in our study it cannot be excluded that the fish were affected by the elevated CO₂, but the effect seems not to have been critical beyond limits of physiological regulation since all fish maintained similar growth rates. This suggests that there could be a critical point of CO₂ concentration between 2000 µatm (this study) and 15,000 µatm (Stiller et al., 2015) where elevated CO₂ begins to affect turbot growth.

4.3 SHORT TERM STUDY (ACUTE CO₂)

Lysozyme is part of the innate immune system and its activity level can be affected by stress (Røed et al., 2002). However, studies have shown different responses of lysozyme following acute and prolonged stress where stress can lead to a reduction as well as an increase in lysozyme activity (Caruso & Lazard, 1999). Chicken egg white lysozyme activity has been found to be influenced by a combination of CO₂ and pH (Banerjee et al., 2011), and Kaya et al. (2014) observed a decrease in lysozyme activity in rainbow trout *Oncorhynchus mykiss* after 7 days of exposure to elevated CO₂, but no

effect was seen after 14 days. However, in the present study, acute exposure led to an increase in lysozyme activity in the high CO₂ treatment. Studies on rainbow trout *Oncorhynchus mykiss* revealed that acute stress triggered the fish's fight or flight response causing an elevated lysozyme activity level (Demers & Bayne, 1997) and gilthead sea bream *Sparus aurata* showed an elevated lysozyme activity after being stressed by aquatic acoustic noise (Filiciotto et al., 2016). This could suggest that elevated CO₂ acted as an immediate stressor in turbot leading to heightened lysozyme activity.

Another important component of the immune system are white blood cells (leukocytes), which consist of cells involved in both innate and adaptive immune response including, but not limited to, monocytes and lymphocytes (Maheswaran et al., 2008, Uribe et al., 2011). Monocytes are phagocytic and are part of the innate immune system whereas lymphocytes are part of adaptive immunity (Uribe et al., 2011). Lymphocytes and monocytes together make up the majority of the lymphatic immune system and therefore analyzing the amount of monocytes and lymphocytes in turbot blood could provide useful insight into the fish immune response. In the short term study, acute CO₂ exposure did not affect the proportion of monocytes and lymphocytes. This suggests that acute CO₂ exposure at projected future oceanic CO₂ levels by end of century and year 2300 (levels used in this experiment) did not trigger an immune response that would alter the amount of leukocytes in turbot.

Gene expression analysis can determine how genes transcribe for synthesis of functional gene product (NCBI, 2014). In this study, gene expression was analyzed by quantifying mRNA levels using methods of real-time PCR (qPCR). The genes of interest consisted of immunity genes (*c3*, *il1b*, *tnfa*, *c1qb*, *cd 8&45*, *cytokin 17*, *cxcl*, *mhcii*, *hep 1&2*, *glys*, *clys*, *tlr3*, *beta-defensin 1&3*, *crp*, *ifn1*, *ifng*, *trans*, *mucin 2&18*, *hsp70*), osmoregulation genes (*ca*, *H⁺-ATPase*), glycolysis genes (*g6p*, *p450*), apoptosis genes (*caspase 3&7*), a tight junction gene (*cadherin*), and an antioxidant gene (*sod*).

Genes involved in osmoregulation in gills (*ca* and *v-type H⁺-ATPase*) were not affected by elevated CO₂ levels during the short term study. This was against initial expectations since various studies have found a change in osmoregulating gene activity after exposure to elevated CO₂ levels in fish (Heuer & Grosell, 2014) such as Atlantic cod

Gadus morhua (Melzner et al., 2009) and rainbow trout *Oncorhynchus mykiss* (Kaya et al., 2013; Lin & Randall, 1993). However, the effect on Atlantic cod in Melzner et al. (2009) was observed at higher CO₂ concentration (~6000 µatm) than this study and no effect was seen at ~3000 µatm. This suggests that turbot's can maintain their acid-base regulation under CO₂ levels used in this experiment, possibly due to the turbot's natural habitat of coastal shallow waters (Froese & Pauly, 2015) where CO₂ fluctuation is naturally present.

In all other organs tested (head kidney, spleen, skin) genes involved in osmoregulation, glycolysis, and most genes in immunity were also not affected by elevated CO₂. *Hepcidin 1*, an innate immunity gene, was down regulated in both head kidney and spleen in the highest CO₂ treatment. *Hep1* is an anti-microbial peptide (Rodrigues et al., 2006) and decrease in *hep1* regulation could impact the fish's ability to fight off bacterial infections. A decrease in *hep1* could be a result from the increase in lysozyme observed in the high CO₂ treatment in this study. Similarly, a study conducted on red porgy *Pagrus pagrus* demonstrated that an increase in lysozyme was linked to a decrease in other immune indicators (Rotllant et al., 1997). This could be due to the increased bactericidal activity of lysozyme (Grinde, 1989; Rainger & Rowley, 1993), which could result in downregulation of *hep1* in form of a negative feedback loop. However, a negative feedback from increase lysozyme might not be the only cause for *hep1* decrease, since a study by Milla et al. (2010) found acute stress to decrease *hepcidin* gene expression as well as lysozyme activity in spleen of Eurasian perch *Perca fluviatilis*. Therefore it is also possible that the energy allocation to lysozyme production led to a decrease in *hep1* production due to less available energy for this pathway. In any case it can be concluded that heightened CO₂ levels of ~2000 µatm decreased levels of *hepcidin 1* and thus might have impaired the antibacterial defense of the fish.

Caspase 3, a pro-apoptotic gene, was down regulated in the high CO₂ treatment in head kidney. *Caspase 3* controls and mediates the fate of cells and is important in apoptosis, an essential process in all organisms' lives to maintain homeostasis (Goodsell, 2000). Head kidney in teleosts composes of mainly leucocytes, and is equivalent to bone marrow of higher vertebrates (Quentel & Obach, 1992). Therefore a decrease in *caspase 3* can impact leukocyte apoptosis and cell turn over, which is an important process to maintain homeostasis (Squier et al., 1995). Evident from the

heightened lysozyme response in the short term study, CO₂ levels in the highest treatment triggered an acute stress response in fish. Stress increases cortisol production (Milla et al., 2010) which in turn, can decrease or inhibit apoptosis (Weyts et al., 1998). The effect of stress on apoptosis inhibition has been witnessed in both fish (Tort, 2011) and in humans (Arimoto et al., 2008). A further investigation to help confirm or reject the link between elevated CO₂ stress and apoptosis inhibition in turbot should analyze cortisol levels under elevated CO₂ conditions.

Superoxide dismutase (*sod*), an antioxidant gene, was found to be upregulated in the spleen of medium CO₂ treatment fish. *Sod* catalyzes superoxide (O₂⁻), a byproduct from metabolic processes, and protects cells against oxidative damage (Zheng et al., 2015). An increase in *sod* could be a response to an increase of free radical O₂⁻ due to acidification. Tomanek et al. (2011) conducted a study on eastern oysters *Crassostrea virginica* and suggested that exposure to elevated CO₂ induces oxidative stress from excess CO₂ interacting with other reactive oxygen species, forming more free radicals. This interaction probably led to the aforementioned upregulation of *sod* in this study. However, the pH optimum of a *sod* enzyme isolated from *Bacillus* sp. was found to be at pH 7.5 (Areekit et al., 2011), which is similar to the pH observed in the high CO₂ treatment of this study. In brine shrimp it was also demonstrated by Zheng et al. (2015) that enzymatic activity of *sod* increased at pH 7.6 (similar to high treatment pH in this study) compared to pH 7.8 (similar to medium treatment pH in this study) and control pH 8.2. Therefore it is possible that the *sod* protein in turbot has an optimal pH around 7.6 as well. This might explain why *sod* was not upregulated in the high CO₂ treatment, as the increase in enzyme activity required less enzyme to be produced.

Cadherin is important in cell adhesion and forming tight junctions to bind cells together (Fuchs & Raghavan, 2002). Since fish skin is directly exposed to surrounding waters, tight junction genes in skin can impact osmoregulation in fish. Studies on *claudin*, another group of tight junction genes, have shown that expression of some *claudin* genes can alter epithelial tightness or permeability (Bagherie-Lachidan et al., 2009). A previous study by Bonga (1997) found that stressors can increase permeability of fish surface epithelia to water and ions. Therefore, the explanation for the upregulation of *cadherin* in turbot skin of the high CO₂ treatment could be to increase cellular adhesions within an already stressed and highly permeable skin in order to

decrease the amount of excess CO₂ entering the body. An alternative reason could be that turbot can sense the increase CO₂ in the water and upregulate *cadherin* as a prevention mechanism against excess CO₂. Not much is known about fish *cadherin* response to elevated CO₂ yet, therefore further investigation into skin structure and permeability in high CO₂ conditions could yield interesting results.

In conclusion, acute CO₂ exposure of 1 week induced a stress response in juvenile turbot, evident in increased lysozyme, inhibited apoptosis (*caspase 3*), and decreased *hep 1* production, while the increase in CO₂ itself heightened anti-oxidation (*sod*) and skin tight junctions (*cadherin*). However, CO₂ exposure at levels in this study did not affect osmoregulation and most immunity genes tested, and nor was growth affected.

4.4 LONG TERM STUDY (CHRONIC CO₂)

Overall, lysozyme activity was not affected by chronic exposure to CO₂. However, a trend to reduced lysozyme activity in the high treatment during week 6 to 10 was indicated. Studies have shown that chronic stress acts as an immunosuppressor in fish (Yin et al., 1995; Möck & Peters, 1990). This suggests that CO₂ in this study acted as an immunosuppressive stressor that gradually affected the turbot, which resulted in a decrease in lysozyme in week 6 and week 10 of the long term experiment. However, turbot were able to acclimatize and were no longer stressed by elevated CO₂ levels, evident in lysozyme levels rising back to Control treatment level at the end of the experiment.

Lysozyme amounts overall were also observed to increase towards the end of the experiment. Comparison between the lysozyme and water temperature graph displayed a similar pattern of sharp increase between week 6 to week 8, suggesting that the sudden increase of lysozyme could be due to stress from elevated temperatures. The increase of lysozyme in the last week could be due to either high temperatures, as seen from the temperature profile, or stress from handling before anaesthetization. Since turbot at sizes used in this experiment (>100g) have an optimum temperature of 16-17°C (Irwin et al., 1999) the water temperature of up to 17-20°C from week 8 - week 16 could have been a stressor to the fish. Again, an analysis of cortisol levels could determine if temperature stress was indeed a cause for these results.

As for blood cell composition in the long term study, no CO₂ effect or time effect on the proportion of monocytes and lymphocytes was found, except for the last week. In week 16, an increase in lymphocytes and decrease in monocytes was observed in the medium CO₂ treatment. In this study, lymphocytes and monocytes were analyzed as relative proportions out of 1.0 or 100% of total live cells. Therefore a change in cell amount of one cell type could influence the proportion of the other. From the results, we cannot conclude whether lymphocytes increased significantly causing the proportion values of monocytes to decrease, or vice versa. If lymphocytes increased, this could be due to temperature increase in the final weeks of the experiment. Studies on fish immunity have found that leucocytes are dependent on environmental temperatures (Alcorn et al., 2002; Martins et al., 2011; Langston et al., 2002). High temperature of ~20°C (compared to ~11°C at start of experiment) coupled with stress from elevated CO₂ could result in an increase in lymphocytes in the final week. Though leucocytes are composed of both lymphocytes and monocytes, which should both display a similar pattern, lymphocytes are known to be more abundant than monocytes (Langston et al., 2002) and therefore a large increase in lymphocytes could mask the smaller increase in monocytes when calculated as proportions or percentage.

Results in gene expression revealed that osmoregulation genes (*ca* and *v-type H⁺-ATPase*) in gills were not affected by elevated CO₂ levels during chronic exposure. Similar to the short term study, this was against expectations, suggesting that turbot acid-base regulation can cope with CO₂ levels in this study.

In head kidney, spleen, and skin, all analyzed genes involved in immune response (*c3*, *il1b*, *tnfa*, *c1qb*, *cd8*, *cytokin 17*, *cxc*, *mhci*, *cd45*, *hep1&2*, *glys*, *clys*, *tlr3*, *beta-defensin1&3*, *crp*, *ifn1*, *ifng*, *trans*, *mucin 2 & 18*, *hsp70*), osmoregulation (*ca* & *H⁺-ATPase*), antioxidant (*sod*), tight junction (*cadherin*), and glycolysis (*g6p* & *p450*) were not affected by elevated CO₂ levels. *Caspase 3*, an apoptosis gene, was also not affected by CO₂. However, *caspase 7*, which is in the same protein family as *caspase 3*, was down regulated in head kidney of high CO₂ treated fish. Since *caspase 7* is involved in apoptosis similar to *caspase 3* mentioned in the short term study, chronic CO₂ exposure could also inhibit apoptosis as suggested earlier. However, it is interesting that two different caspase genes were affected in the short term and long term study. This could

suggest that acute and chronic stress have different pathways in inhibiting turbot cell apoptosis.

Apart from *caspase 7*, *mucin 2* was also affected by CO₂ in turbot head kidney. *Mucin 2* was down regulated in the medium CO₂ treatment. There are two types of mucins, secreted mucins and membrane-associated mucins (Voynow & Rubin, 2009). *Mucin 2* in common carp *Cyprinus carpio* L. is a mucin secreted by epithelial cell and is involved in mucus production (Marel et al., 2012). The fact, however, that *mucin 2* in this study was upregulated in head kidney indicates a different function in turbot. It is possible that turbot *mucin 2* is a membrane-bound mucin, which might be involved in cell signaling and pathogen recognition (Voynow & Rubin, 2009). This indicates that future studies, not only on the effect of CO₂ on mucus production and *mucin* gene expression, but also a deeper characterization of mucins in fish are needed.

Gene expression comparison illustrated a time effect on some genes in gills, head kidney and spleen. In gills, *v-type H⁺-ATPase* of the medium CO₂ treatment displayed a time effect between the short term and long term study of the same treatment. It is interesting that although a time effect on *H⁺-ATPase* gene expression was observed, no treatment or time effect on *ca* gene expression under the same conditions was found. It is possible that the increase in temperature over time of the experiment (~9°C) led to an increase in *ATPase* activity, therefore less amount of enzyme is required to be produced in the long term study. This is observed in the medium CO₂ treatment with a similar pattern displayed in the Control treatment, though statistically not significant. This effect is in agreement to a study on *Na⁺-K⁺-ATPase* that found a much lower *ATPase* activity in winter compared to summer in crucian carp *Carassius carassius* due to temperature differences (Vornanen & Paajanen, 2006). However, *H⁺-ATPase* gene expression in the high CO₂ group remained similar in both short and long term studies despite the temperature increase, which might be due to the need for more *H⁺-ATPase* proteins, for example, a study by Lin & Randall (1993) stated that a 70% increase in *H⁺-ATPase* activity was needed in rainbow trout during hypercapnia treatments. The time effect of *H⁺-ATPase* could also be due to acclimation of turbots to elevated CO₂ during chronic exposures, therefore no longer needing as much osmoregulation as in the short term experiment. Another possibility why this effect was not seen in the high CO₂ treatment could be that fish have alternative excretion pathways for higher CO₂

concentrations, using different proteins and/or different organs for regulations at different stress levels. Other osmoregulation proteins such as *NBC* and *NHE* (Gilmour & Perry, 2009; Heuer & Grosell, 2014; Claiborne et al., 2002), and osmoregulation organs, i.e. kidney, were not analyzed in this study. Therefore an osmoregulatory effect in the high CO₂ treatment could have been missed.

The time effect of head kidney and spleen gene expression was possibly caused by temperature, which was the only abiotic factor that varied in this experiment and affected all treatments. As previously mentioned, the high temperatures occurring in the last half of the experiment (17-20°C) could have been a stressor on the turbot since their optimum temperature is 16-17°C (Irwin et al., 1999). However, because no effect of CO₂ was witnessed between the treatments, the effect is most likely from only temperature stress. Evident from various studies that have shown that gene expression can be influenced by internal and external environmental factors such as temperature (Lobo, 2008; Lo et al., 2006; Whitehead & Crawford, 2006).

Unlike hypothesized from studies that observed an effect of ocean acidification on invertebrate's immune response, such as the green sea urchin *Strongylocentrotus droebachiensis*, a sea star *Leptasterias polaris*, the blue mussel *Mytilus edulis*, and the Norway lobster *Nephrops norvegicus* (Bibby et al., 2008; Dupont & Thorndyke 2012; Hernroth et al., 2012) most immune related genes in turbot were not affected by elevated CO₂. This study revealed that acute exposure to ~2000 µatm CO₂ triggers a stress response in turbot, which leads to an increase in lysozyme, and in turn decreases *hepcidin1* production. Further studies will have to elucidate if this affects the antibacterial defense mechanism. However, no CO₂ stress related effect was found during long term CO₂ exposure, suggesting an acclimation ability of juvenile turbot to hypercapnia. It was also of interest that CO₂ affected other groups of genes, especially apoptosis genes, in spleen and head kidney in both experiments. Future research on a comparative study with other fish species, especially from different natural habitats is needed.

Our results also indicate that natural seasonal temperature coupled with CO₂ can act as a combined stressor and influence turbot immune responses and gene expression. This is important to keep in mind since the IPCC (2014) has predicted an

increase in global sea surface temperature of up to 2-4 °C by the end of century. Since current seasonal temperatures can affect turbot immune responses, the effect of climate change that will threaten turbot might not be ocean acidification but rather sea surface temperature rise.

Scale Properties

Turbot scales are biomineralized structures (Zylberberg et al., 2003; Murcia et al., 2015) and can therefore be affected by ocean acidification similar to other calcifying organisms and impact fish health. It is therefore essential to study the effects of elevated CO₂ levels on the growth and properties of these scales.

The comparison of Young's modulus values of turbot tubercles revealed that no significant effect of CO₂ was observed, with a similar result seen in the hardness values of the scales which also did not differ between treatments. Though studies have shown that CO₂ can impact the inner structure of biomineralized materials (Gutowska et al., 2010), no immediate effect was seen from the modulus and hardness values of the turbot tubercles. This could be due to various reasons. It could be that CO₂ levels used in this study (~1000-2000 µatm) did not impact turbot biomineralizing rate, or turbot were able to acclimatize during 16 weeks of exposure. Another reason could be that measurement indentations were not made on areas that grew during the experiment, rather on pre-existing areas which existed before exposure to CO₂. Since turbot tubercle growth rate is not yet well studied, it is not known how much the scales grew within the 4 months of the experiment

Though unexpected, the findings of scale properties in this experiment are not improbable. Studies on other calcifying organisms have shown that under elevated CO₂, common cuttlefish *Sepia officinalis* maintained growth and calcification (Gutowska et al., 2008), bryozoan *Electra pilosa* increased in growth rates (Saderne & Wahl, 2012), common limpet *Patella vulgate*, barnacle *Semibalanus balanoids*, blue mussel *Mytilus edulis* calcifications remained constant (Findlay, 2011), and brittle star *Amphiura filiformis* increased in calcification rates (Wood et al., 2008). Studies also have shown that CO₂ alone might not impact calcification rates as much as when coupled with other stressors such as food availability as seen in blue mussel (Melzner et al., 2011; Thomsen et al., 2013).

Even though no effect was seen from this study, nanoindentation of turbot scales can still yield useful information on the properties of dry scales, since this was the first study to analyze scale mechanical properties in turbot. The results acquired from this study can contribute to existing knowledge of other fish scale properties. For example, common sole *Solea solea* has a spine modulus of 14 GPa and hardness of 0.4 GPa, while the scale reverse side has a modulus of 3.7 GPa and hardness of 0.14 (Chen et al., submitted manuscript, 2015). Arapaima *Arapaima gigas* scale has an external layer hardness of 2 GPa and internal layer hardness of 0.6 GPa (Lin et al., 2011), and gray bichir *Polypterus senegalus* has a scale hardness from inner to outer surface between 0.54-4.5 GPa (Bruet et al., 2008). In relation to these findings, dry turbot tubercle, which was measured from the upside growth region (Young's modulus ~5 GPa, hardness ~0.16 GPa) seems to have a similar hardness to the reverse scale side of *S. solea* which is lower than *S. solea* spine, *A. gigas*, and *P. senegalus* hardness.

It is noteworthy that Kiel Fjord and the Baltic sea water fluctuates in CO₂ levels and has known to previously reach up to 3000 µatm (Thomsen et al., 2013) which exceeds this experiment's highest CO₂ treatment. Turbots used in this experiment were reared in ambient Kiel Fjord water prior to the experiment, so if they have previously been exposed to elevated CO₂, it could affect their ability to acclimatize to CO₂ treatments used in this study. Also worth noting is that the natural habitat of turbot is in coastal shallow waters (Froese & Pauly, 2015), which can reach much higher pCO₂ values than the open ocean (Melzner et al., 2013). In the same order of flatfishes, Atlantic halibut *Hippoglossus hippoglossus* in aquaculture (Daniels & Watanabee, 2010) can tolerate CO₂ levels of up to 20 mg/L or ~12,000 µatm. Therefore, and this is corroborated by results from this study, turbot might have a precondition to tolerate elevated CO₂ levels up to a critical point.

5. CONCLUSION

In conclusion, juvenile turbot's immune response and scale properties in this experiment were not severely affected by CO₂ levels predicted for the future ocean. From our results it can be predicted that juvenile turbot will be able to acclimate to CO₂ levels as projected for the future open ocean. In regard to recirculating aquaculture situations however our results together with the study by Stiller et al. (2015) suggest that optimal and maximum CO₂ levels have to be defined to insure fish welfare and optimal production output.

ACKNOWLEDGEMENT

This thesis was partly funded by the project FINE-Aqua in co-operation with GEOMAR Helmholtz Centre for Ocean Research Kiel and Kiel University (CAU). I would like to thank all my supervisors, Joanna, Marlene, Catriona, Prof. Reusch, and Prof. Gorb for this thesis opportunity and the advices you have all given me. A special thanks to Joanna for going above and beyond being my supervisor and spending almost every day of my experiment with me. Thank you to everyone else that has helped me through this experiment which would not have finished without these people, Isabel Keller, Alexander Kovalev, Fabian Wendt, Martin Grimm, Diana Gill, Claas Hiebenthal, Svend Mees, Diana Gill, Felix Mittermayer, Ulrike Panknin, Janina Büscher, Jasha Dehm, Manuel Olivares Requena, and Maude Poirier.

A big thank you to my friends who have supported me along the way and procrastinated with me with lunches and coffee. Last but not least, thanks to my family who have always supported me through years of living across continents and called every week to check up on me and my thesis.

REFERENCES

- Amend, D., & Smith, L. (1975). Pathophysiology of infectious hematopoietic necrosis virus disease in rainbow trout: hematological and blood chemical changes in moribund fish. *Infection and immunity*, *11*(1), 171–9.
- Areekit, S., Kanjanavas, P., Khawsak, P., Pakpitchareon, A., Potivejkul, K., Chansiri, G., & Chansiri, K. (2011). Cloning, expression, and characterization of thermotolerant manganese superoxide dismutase from *Bacillus* sp. MHS47. *International journal of molecular sciences*, *12*(1), 844–56.
- Arimoto, K., Fukuda, H., Imajoh-Ohmi, S., Saito, H., & Takekawa, M. (2008). Formation of stress granules inhibits apoptosis by suppressing stress-responsive MAPK pathways. *Nature Cell Biology* *10*, 1324 – 1332.
- Bagherie-Lachidan, M., Wright, S.I., & Kelly, S.P. (2009). Claudin-8 and-27 tight junction proteins in puffer fish *Tetraodon nigroviridis* acclimated to freshwater and seawater. *Journal of Comparative Physiology B*, *179*(4), 419–431.
- Banerjee, P., Keener, K., & Lukito, V. (2011). Influence of carbon dioxide on the activity of chicken egg white lysozyme. *Poultry science*, *90*(4), 889–95.
- Barton, B.A., Morgan, J.D., & Vijayan, M.M. (2002). Physiological and condition-related indicators of environmental stress in fish. *Biological indicators of aquatic ecosystem stress* (pp. 111–148). Bethesda USA: American Fisheries Society.
- Bibby, R., Widdicombe, S., Parry, H., Spicer, J., & Pipe, R. (2008). Effects of ocean acidification on the immune response of the blue mussel *Mytilus edulis*. *Aquatic Biology*, *2*, 67–74.
- Bonga, S.E.W. (1997). The stress response in fish. *Physiological Reviews*, *77*(3), 591–625.
- Bruet, B.J.F., Song, J., Boyce, M.C., & Ortiz, C. (2008). Materials design principles of ancient fish armour. *Nature Materials*, *7*, 748 – 756.
- Budy, P., Baker, M., & Dahle, S. (2011). Predicting fish growth potential and identifying water quality constraints: A spatially-explicit bioenergetics approach. *Environmental Management*, *48*(4), 691–709.
- Caldeira, K., & Wickett, M.E. (2003). Oceanography: anthropogenic carbon and ocean pH. *Nature*, *425*(6956), 365.
- Caruso, D., & Lazard, J. (1999). Subordination stress in Nile tilapia and its effect on plasma lysozyme activity. *Journal of Fish Biology*, *55*(2), 451–454.
- Chen, P.-Y., Schirer, J., Simpson, A., Nay, R., Lin, Y.-S., Yang, W., Lopez, M. I., Li, J., Olevsky, E.A., & Meyers, M.A. (2012). Predation versus protection: fish teeth and scales evaluated by nanoindentation. *Journal of Materials Research*, *27*(01), 100–112.
- Chen, S.M., Gorb, S.N., Kovalev, A., & Spinner, M. (2015). Structure and mechanical properties of the ctenoid scales of the burying flatfish *Solea solea* (Osteichthyes, Pleuronectiformes). Manuscript submitted for publication.
- Claiborne, J., Edwards, S., & Morrison-Shetlar, A. (2002). Acid–base regulation in fishes: cellular and molecular mechanisms. *Journal of Experimental Zoology*, *293*(3), 302–319.

- Daniels, H.V., & Watanabe, W.O. (Eds.) (2010). *Practical flatfish culture and stock enhancement*. Singapore: Blackwell Publishing.
- Demers, N., & Bayne, C. (1997). The immediate effects of stress on hormones and plasma lysozyme in rainbow trout. *Developmental & Comparative Immunology*, 21(4), 363-373.
- Dickson, A.G., Sabine, C.L., & Christian, J.R. (2007). Guide to best practices for ocean CO₂ measurements. *PICES Special Publication*, 3, 191 pp.
- Doney, S.C., & Levine, N.M. (2006). "How Long Can the Ocean Slow Global Warming?". *Oceanus*. Woods Hole Oceanographic Institution. Retrieved from www.whoi.edu/oceanus.
- Dupont, S., & Thorndyke, M. (2012). Relationship between CO₂-driven changes in extracellular acid–base balance and cellular immune response in two polar echinoderm species. *Journal of Experimental Marine Biology and Ecology*, 424-425, 3237.
- Exadactylos, A., Rigby, M.J., Geffen, A.J., & Thorpe, J.P. (2007). Conservation aspects of natural populations and captive-bred stocks of turbot (*Scophthalmus maximus*) and Dover sole (*Solea solea*) using estimates of genetic diversity. *ICES Journal of Marine Science*, 64, 1173-1181.
- Fabry, V., Seibel, B., Feely, R., & Orr, J. (2008). Impacts of ocean acidification on marine fauna and ecosystem processes. *ICES Journal of Marine Science: Journal du Conseil*, 65(3), 414–432.
- Faílde, L., Bermúdez, R., Vigliano, F., Coscelli, G., & Quiroga, M. (2014). Morphological, immunohistochemical and ultrastructural characterization of the skin of turbot (*Psetta maxima* L.). *Tissue and Cell*, 46(5), 334-342.
- Faílde, L.D., Losada, A.P., Bermúdez, R., Santos, Y., & Quiroga, M.I. (2014). Evaluation of immune response in turbot (*Psetta maxima* L.) tenacibaculosis: haematological and immunohistochemical studies. *Microbial pathogenesis*, 76, 1–9.
- Feely, R., Sabine, C., Lee, K., Berelson, W., Kleyvas, J., Fabry, V., & Millero, F. (2004). Impact of anthropogenic CO₂ on the CaCO₃ system in the oceans. *Science*, 305(5682), 362-366.
- Filiciotto, F., Cecchini, S., Buscaino, G., Maccarrone, V., Piccione, G., & Fazio, F. (2016). Impact of aquatic acoustic noise on oxidative status and some immune parameters in gilthead sea bream *Sparus aurata* (Linnaeus, 1758) juveniles. *Aquaculture Research*, 1-9.
- Findlay, H., Wood, H., Kendall, M., Spicer, J., Twitchett, R., & Widdicombe, S. (2011). Comparing the impact of high CO₂ on calcium carbonate structures in different marine organisms. *Marine Biology Research*, 7(6), 565–575.
- Froese, R. (2006). Cube law, condition factor and weight–length relationships: history, meta-analysis and recommendations. *Journal of Applied Ichthyology*, 22(4), 241–253.
- Froese, R., & Pauly, D. Editors. (2015). FishBase. World Wide Web electronic publication. www.fishbase.org, (04/2015)
- Frommel, A., Maneja, R., Lowe, D., Malzahn, A., Geffen, A., Folkvord, A., Piatkowski, U., Reusch, T.B.H., & Clemmesen, C. (2011). Severe tissue damage in Atlantic cod larvae under increasing ocean acidification. *Nature Climate Change*, 2(1), 42–46.
- Frommel, A., Maneja, R., Lowe, D., Pascoe, C., Geffen, A., Folkvord, A., Piatkowski, U., & Clemmesen, C. (2014). Organ damage in Atlantic herring larvae as a result of ocean acidification. *Ecological Applications*, 24(5).

- Fuchs, E., & Raghavan, S. (2002). Getting under the skin of epidermal morphogenesis. *Nature reviews. Genetics*, 3(3), 199–209.
- Gilliers, C., Pape, O., Désaunay, Y., Morin, J., Guérault, D., & Amara, R. (2006). Are growth and density quantitative indicators of essential fish habitat quality? An application to the common sole *Solea solea* nursery grounds. *Estuarine, Coastal and Shelf Science*, 69(1-2), 96–106.
- Gilmour, K., & Perry, S. (2009). Carbonic anhydrase and acid-base regulation in fish. *Journal of Experimental Biology*, 212(11), 1647-1661.
- Goodsell, D. (2000). The molecular perspective: Caspases. *Stem Cells*, 18(6), 457–458.
- Gosselin, L.A., & Qian, P.Y. (1997). Juvenile mortality in benthic marine invertebrates. *Marine Ecology Progress Series*, 146, 265-282.
- Greenstreet, S.P.R., & Rogers, S.I. (2006). Indicators of the health of the North Sea fish community: identifying reference levels for an ecosystem approach to management. *ICES Journal of Marine Science*, 63(4), 573–593.
- Grinde, B. (1989). Lysozyme from rainbow trout, *Salmo gairdneri* Richardson, as an antibacterial agent against fish pathogens. *Journal of Fish Diseases*, 12(2), 95-104.
- Grinde, B., Jollès, J., & Jollès, P. (1988). Purification and characterization of two lysozymes from rainbow trout (*Salmo gairdneri*). *European Journal of Biochemistry*, 173(2), 269–273.
- Guinotte, J., & Fabry, V. (2008). Ocean acidification and its potential effects on marine ecosystems. *Annals of the New York Academy of Sciences*, 1134(1), 320–342.
- Gutowska, M., Melzner, F., Pörtner, H., & Meier, S. (2010). Cuttlebone calcification increases during exposure to elevated seawater pCO₂ in the cephalopod *Sepia officinalis*. *Marine Biology*, 157(7), 1653–1663.
- Gutowska, M., Pörtner, H., & Melzner, F. (2008). Growth and calcification in the cephalopod *Sepia officinalis* under elevated seawater pCO₂. *Marine Ecology Progress Series*, 373, 303-309.
- Hammen, T., Poos, J., Overzee, H., Heessen, H., Magnusson, A., & Rijnsdorp, A. (2013). Population ecology of turbot and brill: What can we learn from two rare flatfish species?. *Journal of Sea Research*, 84, 96-108.
- Heuer, R., & Grosell, M. (2014). Physiological impacts of elevated carbon dioxide and ocean acidification on fish. *American Journal of Physiology - Regulatory, Integrative and Comparative Physiology*, 307(9), R1061–R1084.
- Huang, Z., Ma, A., & Wang, X. (2011). The immune response of turbot, *Scophthalmus maximus* (L.), skin to high water temperature. *Journal of Fish Diseases*, 34(8), 619-627.
- Hutchinson, T.H., Solbe, J., & Kloepper-Sams, P.J. (1998). Analysis of the ECETOC Aquatic Toxicity (EAT) Database: III-Comparative toxicity of chemical substances to different life stages of aquatic organisms. *Chemosphere*, 36 (1), 129-142.
- IPCC. (2007). *Climate Change 2007: The physical science basis. Contribution of working group I to the fourth assessment report of the Intergovernmental Panel on Climate Change.* Cambridge University Press, Cambridge, United Kingdom.

- IPCC. (2014). *Climate Change 2014: Impacts, adaptation, and vulnerability. Contribution of working group II to the fifth assessment report of the Intergovernmental Panel on Climate Change*. Cambridge University Press, Cambridge, United Kingdom and New York, NY, USA, 1820 pp.
- Irwin, S., O'Halloran, J., & FitzGerald, R.D. (1999) Stocking density, growth and growth variation in juvenile turbot, *Scophthalmus maximus* (Rafinesque). *Aquaculture*, 178, 78-88.
- Ishimatsu, A., Kikkawa, T., Hayashi, M., Lee, K.-S., & Kita, J. (2004). Effects of CO₂ on marine fish: larvae and adults. *Journal of Oceanography*, 60(4), 731–741.
- Kaya, H., Yilmaz, S., Gürkan, M., & Hisar, O. (2013). Effects of environmental hypercapnia on hemato-immunological parameters, carbonic anhydrase, and Na⁺-K⁺-ATPase enzyme activities in rainbow trout (*Oncorhynchus mykiss*) tissues. *Toxicological & Environmental Chemistry*, 95(8), 1395-1407.
- Ken, C.-F., Lin, C.-T., Shaw, J.-F., & Wu, J.-L. (2003). Characterization of fish Cu/Zn-superoxide dismutase and its protection from oxidative stress. *Marine biotechnology*, 5(2), 167–73.
- Landis, S., Kalbe, M., Reusch, T., & Roth, O. (2012). Consistent pattern of local adaptation during an experimental heat wave in a pipefish-trematode host-parasite system. *PloS one*, 7(1), e30658.
- Langston, A., Hoare, R., Stefansson, M., Fitzgerald, R., Wergeland, H., & Mulcahy, M. (2002). The effect of temperature on non-specific defence parameters of three strains of juvenile Atlantic halibut (*Hippoglossus hippoglossus* L.). *Fish & Shellfish Immunology*, 12(1), 61-76.
- Lin, H., & Randall, D.J. (1993). H⁺-ATPase activity in crude homogenates of fish gill tissue: inhibitor sensitivity and environmental and hormonal regulation. *Journal of Experimental Biology*, 180, 163-174.
- Lin., Y.S., Wei, C.T., Olevsky, E.A., Meyers, M.A. (2011). Mechanical properties and the laminate structure of *Arapaima gigas* scales. *Journal of the Mechanical Behavior of Biomedical Materials*, 4(7), 1145-1156.
- Livak, K. J., & Schmittgen, T.D. (2001). Analysis of relative gene expression data using real-time quantitative PCR and the 2^{-ΔΔCt} method. *Methods*, 25(4), 402–408.
- Lo, M., Bulach, D., Powell, D., Haake, D., Matsunaga, J., Paustian, M., Zuerner, R., & Adler, B. (2006). Effects of temperature on gene expression patterns in *Leptospira interrogans* Serovar Lai as assessed by whole-genome microarrays. *Infection and Immunity*, 74(10), 5848–5859.
- Lobo, I. (2008). Environmental influences on gene expression. *Nature Education*, 1(1), 39.
- Maheswaran, R., Devapaul, A., Muralidharan, S., Velmurugan, B., & Ignacimuthu, S. (2008). Haematological studies of freshwater fish, *Clarias batrachus* (L.) exposed to mercuric chloride. *International Journal of Integrative Biology*, 2(1), 49–54.
- Marel, M., Adamek, M., Gonzalez, S., Frost, P., Rombout, J., Wiegertjes, G., Savelkoul, H., & Steinhagen, D. (2012). Molecular cloning and expression of two β-defensin and two mucin genes in common carp (*Cyprinus carpio* L.) and their up-regulation after β-glucan feeding. *Fish & Shellfish Immunology*, 32(3), 494–501.

- Martins, M., Xu, D., Shoemaker, C., & Klesius, P. (2011). Temperature effects on immune response and hematological parameters of channel catfish *Ictalurus punctatus* vaccinated with live theronts of *Ichthyophthirius multifiliis*. *Fish & shellfish immunology*, 31(6), 774–80.
- Melzner, F., Göbel, S., Langenbuch, M., Gutowska, M., Pörtner, H.-O., & Lucassen, M. (2009). Swimming performance in Atlantic Cod (*Gadus morhua*) following long-term (4–12 months) acclimation to elevated seawater PCO₂. *Aquatic Toxicology*, 92(1), 3037.
- Melzner, F., Stange, P., Trübenbach, K., Thomsen, J., Casties, I., Panknin, U., Gorb, S.N., Gutowska, M.A. (2011). Food supply and seawater pCO₂ impact calcification and internal shell dissolution in the blue mussel *Mytilus edulis*. *PLoS one*, 6(9), e24223.
- Melzner, F., Thomsen, J., Koeve, W., Oschlies, A., Gutowska, M.A., Bange, H.W., Hansen, H.P., & Körtzinger, A. (2013). Future ocean acidification will be amplified by hypoxia in coastal habitats. *Marine Biology*, 160(8), 1875–1888.
- Miest, J., Arndt, C., Adamek, M., Steinhagen, D., & Reusch, T. (2016). Dietary β-glucan (MacroGard®) enhances survival of first feeding turbot (*Scophthalmus maximus*) larvae by altering immunity, metabolism and microbiota. *Fish & Shellfish Immunology*, 48, 94–104.
- Miest, J.J., & Bray, D. (2016). Changes in the chemical profile of infected fish as a potential tool for disease diagnosis. Manuscript in preparation.
- Milla, S., Mathieu, C., Wang, N., Lambert, S., Nadzialek, S., Massart, S., Henrotte, E., Douxfils, J., Mélard, C., Mandiki, S.N.M., Kestemont, P. (2010). Spleen immune status is affected after acute handling stress but not regulated by cortisol in Eurasian perch, *Perca fluviatilis*. *Fish & Shellfish Immunology*, 28(5-6), 931–941.
- Miyazaki, T. (1998). Influences of pH and temperature on lysozyme activity in the plasma of Japanese flounder and Japanese char. *Fish Pathology*, 33(1), 7–10.
- Möck, A. & Peters, G. (1990). Lysozyme activity in rainbow trout, *Oncorhynchus mykiss* (Walbaum), stressed by handling, transport and water pollution. *Journal of Fish Biology*, 37(6), 873–885.
- Munday, P., Cheal, A., Dixon, D., Rummer, J., & Fabricius, K. (2014). Behavioural impairment in reef fishes caused by ocean acidification at CO₂ seeps. *Nature Climate Change*, 4(6), 487–492.
- Murcia, S., McConville, M., Li, G., Ossa, A., & Arola, D. (2015). Temperature effects on the fracture resistance of scales from *Cyprinus carpio*. *Acta biomaterialia*, 14, 154–63.
- Oliver, W.C., & Pharr, G.M. (1992). An improved technique for determining hardness and elastic modulus using load and displacement sensing indentation experiments. *Journal of materials research*, 7(06), 1564–1583.
- Oliver, W.C., & Pharr, G.M. (2004). Measurement of hardness and elastic modulus by instrumented indentation: Advances in understanding and refinements to methodology. *Journal of materials research*, 19, 3–20.
- Pankhurst, N.W. & Van der Kraak, G. (1997). Effects of stress on reproduction and growth of fish. In G.K. Iwama, A.D. Pickering, J.P. Sumpter, & C.B. Schreck (Eds.), *Fish stress and health in aquaculture; Society for experimental biology seminar series 62* (pp. 73–93). Cambridge, UK: Cambridge University Press.

- Pierrot, D., Lewis, E., & Wallace, D.W.R. (2006). MS Excel program developed for CO₂ system calculations. Carbon Dioxide Information Analysis Center, Oak Ridge National Laboratory, U.S. Department of Energy, Oak Ridge, Tennessee.
- Quentel, C., & Obach, A. (1992). The cellular composition of the blood and haematopoietic organs of turbot *Scophthalmus maximus* L. *Journal of Fish Biology*, *41*, 709–716.
- Rainger, G.E., & Rowley, A.F. (1993). Antibacterial activity in the serum and mucus of rainbow trout, *Oncorhynchus mykiss*, following immunisation with *Aeromonas salmonicida*. *Fish & Shellfish Immunology*, *3*(6), 475-482.
- Rakers, S., Gebert, M., & Uppalapati, S. (2010). “Fish matters”: the relevance of fish skin biology to investigative dermatology. *Experimental Dermatology*, *19*, 313-324.
- Riebesell, U., Zondervan, I., Rost, B., Tortell, P., Zeebe, R., & Morel, F. (2000). Reduced calcification of marine plankton in response to increased atmospheric CO₂. *Nature*, *407*(6802), 364–367.
- Rodrigues, P., Vázquez-Dorado, S., Neves, J., & Wilson, J. (2006). Dual function of fish hepcidin: response to experimental iron overload and bacterial infection in sea bass (*Dicentrarchus labrax*). *Developmental and comparative immunology*, *30*(12), 1156–67.
- Rotllant, J., Pavlidis, M., Kentouri, M., Abad, M., & Tort, L. (1997). Non-specific immune responses in the red porgy *Pagrus pagrus* after crowding stress. *Aquaculture*, *156*(3-4), 279–290.
- Røed, K., Fevolden, S.-E., & Fjalestad, K. (2002). Disease resistance and immune characteristics in rainbow trout (*Oncorhynchus mykiss*) selected for lysozyme activity. *Aquaculture*, *209*(1- 4), 91–101.
- Saderne, V., & Wahl, M. (2012). Effect of ocean acidification on growth, calcification and recruitment of calcifying and non-calcifying epibionts of brown algae. *Biogeosciences Discussions*, *9*, 3739-3766.
- Sæther, B., & Jobling, M. (1999). The effects of ration level on feed intake and growth, and compensatory growth after restricted feeding, in turbot *Scophthalmus maximus* L. *Aquaculture Research*, *30*(9), 647–653.
- Souza, K., Jutfelt, F., Kling, P., Förlin, L., & Sturve, J. (2014). Effects of increased CO₂ on fish gill and plasma proteome. *PLoS ONE*, *9*(7).
- Squier, M.K.T., Sehnert, A.J., & Cohen, J.J. (1995). Apoptosis in leukocytes. *Journal of Leukocyte Biology*, *57*, 2-10.
- Stiller, K., Vanselow, K., Moran, D., Bojens, G., Voigt, W., Meyer, S., & Schulz, C. (2015). The effect of carbon dioxide on growth and metabolism in juvenile turbot *Scophthalmus maximus* L. *Aquaculture*, *444*, 143150.
- Stiller, K., Moran, D., Vanselow, K., Marxen, K., Wuertz, S., & Schulz, C. (2013). A novel respirometer for online detection of metabolites in aquaculture research: Evaluation and first applications. *Aquacultural Engineering*, *55*, 23-31.
- Thomsen, J., Casties, I., Pansch, C., Körtzinger, A., & Melzner, F. (2013). Food availability outweighs ocean acidification effects in juvenile *Mytilus edulis*: laboratory and field experiments. *Global change biology*, *19*(4), 1017–27.
- Tort, L. (2011). Stress and immune modulation in fish. *Developmental and comparative immunology*, *35*(12), 1366–75.

- Uribe, C., Folch, H., Enriquez, R., & Moran, G. (2011). Innate and adaptive immunity in teleost fish: a review. *Veterinarni Medicina*, 56(10), 486-503.
- Van Weerd, J.H., & Komen, J. (1998). The effects of chronic stress on growth in fish: a critical appraisal. *Comparative Biochemistry and Physiology Part A: Molecular & Integrative Physiology*, 120(1), 107-112.
- Viadero, R.C. (2005). Factors affecting fish growth and production. *Water Encyclopedia*, 3, 129-133.
- Vornanen, M., & Paajanen, V. (2006). Seasonal changes in glycogen content and Na⁺-K⁺-ATPase activity in the brain of crucian carp. *American journal of physiology. Regulatory, integrative and comparative physiology*, 291(5), R1482-9.
- Voynow, J.A. & Rubin, B.K. (2009). Mucins, mucus, and sputum. *Chest*, 135(2), 505-512.
- Weyts, F.A., Flik, G., & Kemenade, B.M.L.V. (1998). Cortisol inhibits apoptosis in carp neutrophilic granulocytes. *Developmental & Comparative Immunology*, 22(5-6), 563-572.
- Whitehead, A., & Crawford, D. (2006). Neutral and adaptive variation in gene expression. *Proceedings of the National Academy of Sciences of the United States of America*, 103(14), 5425-30.
- Wood, H., Spicer, J., & Widdicombe, S. (2008). Ocean acidification may increase calcification rates, but at a cost. *Proceedings of the Royal Society B: Biological Sciences*, 275(1644), 1767-1773.
- Yin, Z., Lam, T.J., & Sin, Y.M. (1995). The effects of crowding stress on the non-specific immuneresponse in fancy carp (*Cyprinus carpio* L.). *Fish & Shellfish Immunology*, 5, 519-529.
- Zhang, Y., Mai, K., Ma, H., Ai, Q., Zhang, W., & Xu, W. (2011). Rearing in intermediate salinity enhances immunity and disease-resistance of turbot (*Scophthalmus maximus* L.). *Acta Oceanologica Sinica*, 30(4), 122128.
- Zheng, C., Jeswin, J., Shen, K., Lablche, M., Wang, K., & Liu, H. (2014). Detrimental effect of CO₂-driven seawater acidification on a crustacean brine shrimp, *Artemia sinica*. *Fish & shellfish immunology*, 43(1), 181-90.
- Zylberberg, L., Chanet, B., Wagemans, F., & Meunier, F. (2003). Structural peculiarities of the tubercles in the skin of the turbot, *Scophthalmus maximus* (L., 1758) (Osteichthyes, Pleuronectiformes, Scophthalmidae). *Journal of Morphology*, 258(1), 84-96.

APPENDIX

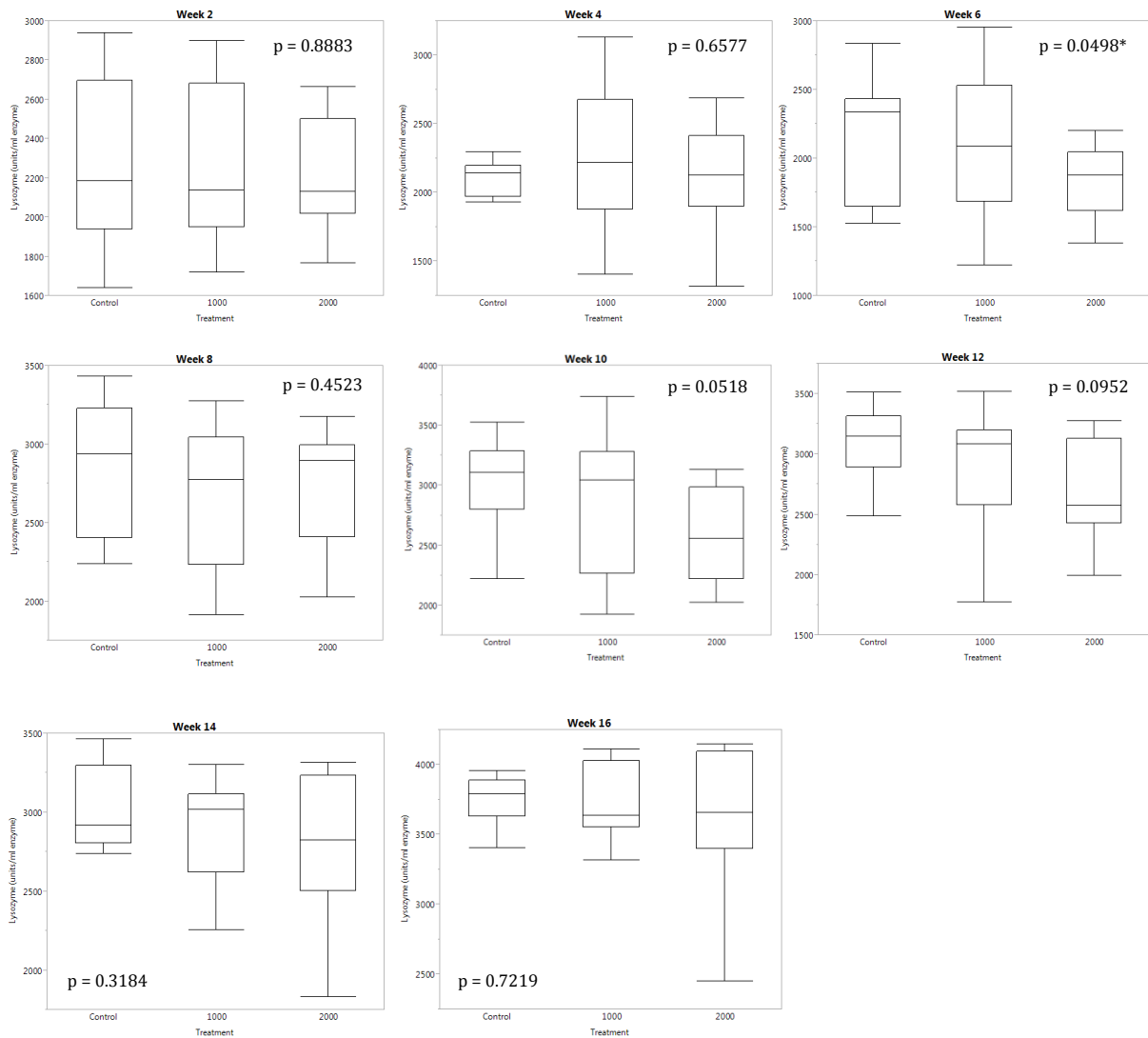


Figure A1: Box plot of bi-weekly mean lysozyme activity with ANOVA p-values in turbot serum in 16 week experiment. Box plot shows median, upper and lower quartile, minimum and maximum.

Table A1: Mean lysozyme activity (units/ml enzyme) ± SEM in 16 week experiment turbot serum

Time	Lysozyme activity (units/ml enzyme)			p-value
	Control	Medium CO ₂	High CO ₂	
Week 2	2290±129	2289±121	2222±84	0.8883
Week 4	2001±77	2250±150	2104±113	0.6577
Week 6	2151±123	1940±224	1825±73	0.0498
Week 8	2876±124	2665±127	2732±110	0.4523
Week 10	3043±111	2869±169	2568±112	0.0518
Week 12	3080±84	2910±148	2693±124	0.0952
Week 14	3019±76	2788±148	2775±143	0.3184
Week 16	3750±53	3578±156	3617±157	0.7219

Table A2: *ca* and *H⁺-ATPase* gene expression values ± SEM in turbot gills of short term and long term experiment

Genes	Experiment	Gene Expression	Control	Medium CO ₂	High CO ₂
CA	1 Week	Relative to Control (x-fold)	1.05±0.11	1.15±0.21	0.99±0.19
		ΔCt	1.57±0.14	1.59±0.26	1.83±0.26
	16 Week	Relative to Control (x-fold)	1.02±0.06	1.19±0.21	1.16±0.15
		ΔCt	1.60±0.09	1.60±0.26	1.56±0.26
H ⁺ -ATPase	1 Week	Relative to Control (x-fold)	1.13±0.15	1.12±0.07	1.13±0.14
		ΔCt	7.13±0.24	6.99±0.09	7.08±0.18
	16 Week	Relative to Control (x-fold)	1.03±0.08	0.98±0.08	1.29±0.15
		ΔCt	7.51±0.11	7.61±0.15	7.24±0.18

Table A3: Δ Ct gene expression values \pm SEM of time effected genes in turbot head kidney

Gene	1 Week			16 Week			ANOVA (df=1)
	Control	Medium CO ₂	High CO ₂	Control	Medium CO ₂	High CO ₂	
C3	10.13 \pm 0.54	9.15 \pm 0.88	8.55 \pm 0.24	7.79 \pm 0.50	8.14 \pm 0.69	7.65 \pm 0.43	F = 9.44 p = .0031
CA	1.06 \pm 0.09	1.14 \pm 0.12	1.13 \pm 0.10	0.36 \pm 0.20	0.35 \pm 0.14	0.54 \pm 0.14	F = 26.52 p <.0001
Caspase3	4.79 \pm 0.09	4.98 \pm 0.12	5.13 \pm 0.08	4.13 \pm 0.14	4.40 \pm 0.10	4.33 \pm 0.24	F = 45.88 p <.0001
GAPDH	1.22 \pm 0.12	1.64 \pm 0.29	1.58 \pm 0.14	0.74 \pm 0.38	0.66 \pm 0.40	0.49 \pm 0.30	F = 18.71 p <.0001
gLys	3.06 \pm 0.13	2.95 \pm 0.12	3.22 \pm 0.14	2.26 \pm 0.15	2.64 \pm 0.16	2.58 \pm 0.14	F = 25.76 p <.0001
SOD	2.36 \pm 0.13	2.45 \pm 0.12	2.50 \pm 0.13	0.87 \pm 0.15	1.22 \pm 0.24	1.34 \pm 0.19	F = 80.51 p <.0001

Table A4: Δ Ct gene expression values \pm SEM of time effected genes in turbot spleen

Gene	1 Week			16 Week			ANOVA (df=1)
	Control	Medium CO ₂	High CO ₂	Control	Medium CO ₂	High CO ₂	
C1qB	0.82 \pm 0.13	0.84 \pm 0.10	0.82 \pm 0.08	-0.26 \pm 0.20	-0.39 \pm 0.13	-0.09 \pm 0.17	F = 90.19 p <.0001
CA	0.18 \pm 0.21	0.18 \pm 0.24	0.54 \pm 0.18	-1.48 \pm 0.11	-1.25 \pm 0.14	-1.27 \pm 0.08	F = 151.0 p <.0001
Caspase3	6.54 \pm 0.10	6.36 \pm 0.14	6.76 \pm 0.10	4.67 \pm 0.27	5.59 \pm 0.38	5.30 \pm 0.21	F = 59.13 p <.0001
GAPDH	2.86 \pm 0.19	3.37 \pm 0.20	3.27 \pm 0.18	2.05 \pm 0.17	1.87 \pm 0.10	2.23 \pm 0.11	F = 54.68 p <.0001
gLys	2.86 \pm 0.08	2.81 \pm 0.10	3.09 \pm 0.07	1.68 \pm 0.19	2.01 \pm 0.19	2.06 \pm 0.21	F = 68.55 p <.0001
IL1b	9.45 \pm 0.23	9.54 \pm 0.16	9.49 \pm 0.20	7.42 \pm 0.31	7.16 \pm 0.19	7.36 \pm 0.39	F = 85.68 p <.0001
SOD	2.99 \pm 0.07	2.68 \pm 0.09	3.26 \pm 0.14	1.53 \pm 0.34	1.88 \pm 0.24	1.91 \pm 0.22	F = 25.04 p <.0001
TLR3	7.43 \pm 0.29	6.92 \pm 0.27	7.04 \pm 0.31	5.25 \pm 0.32	5.27 \pm 0.22	5.39 \pm 0.31	F = 55.17 p <.0001
cLys	5.47 \pm 0.71	6.06 \pm 0.54	5.79 \pm 0.54	6.69 \pm 0.56	7.56 \pm 0.43	6.95 \pm 0.62	F = 15.75 p =.0002
G6P	12.20 \pm 0.54	12.58 \pm 0.48	12.08 \pm 0.58	15.50 \pm 0.39	16.05 \pm 0.70	15.12 \pm 0.44	F = 59.93 p <.0001
Hep2	10.16 \pm 0.97	10.77 \pm 0.88	10.24 \pm 0.64	13.07 \pm 0.93	14.10 \pm 0.75	12.86 \pm 0.66	F = 30.39 p <.0001
MHCII	1.13 \pm 0.24	1.80 \pm 0.20	1.26 \pm 0.41	3.16 \pm 0.69	2.32 \pm 0.39	1.93 \pm 0.38	F = 11.09 p =.0014
Mucin18	6.78 \pm 0.14	7.28 \pm 0.14	7.25 \pm 0.19	7.49 \pm 0.18	7.70 \pm 0.18	7.82 \pm 0.18	F = 19.40 p <.0001
Trans	8.71 \pm 0.85	9.26 \pm 0.52	9.81 \pm 0.60	11.49 \pm 0.56	12.38 \pm 0.53	11.11 \pm 0.59	F = 35.40 p <.0001

Table A5: Amount of lymphocytes proportion (relative to live cells) \pm SEM in fresh turbot blood from 16 week experiment with ANOVA

Time	Lymphocytes proportion (relative to live cells)			Statistics (df=2)
	Control	Medium CO ₂	High CO ₂	
Week 2	0.64 \pm 0.02	0.68 \pm 0.02	0.65 \pm 0.01	F=0.0547, p=0.9468
Week 4	0.61 \pm 0.02	0.62 \pm 0.02	0.65 \pm 0.02	F=1.0702, p=0.3553
Week 6	0.69 \pm 0.01	0.67 \pm 0.02	0.68 \pm 0.01	F=0.3530, p=0.7053
Week 8	0.74 \pm 0.02	0.72 \pm 0.02	0.67 \pm 0.05	F=1.2730, p=0.2963
Week 10	0.64 \pm 0.01	0.66 \pm 0.02	0.65 \pm 0.01	F=0.3798, p=0.6871
Week 12	0.70 \pm 0.02	0.69 \pm 0.03	0.72 \pm 0.01	F=0.1428, p=0.8675
Week 14	0.71 \pm 0.02	0.69 \pm 0.01	0.72 \pm 0.01	F=0.9451, p=0.3992
Week 16	0.66 \pm 0.02	0.74 \pm 0.02	0.67 \pm 0.02	F=4.6742, p=0.0163

Table A6: Amount of monocytes proportion (relative to live cells) \pm SEM in fresh turbot blood from 16 week experiment with ANOVA

Time	Monocytes proportion (relative to live cells)			Statistics (df=2)
	Control	Medium CO ₂	High CO ₂	
Week 2	0.46 \pm 0.02	0.43 \pm 0.03	0.45 \pm 0.02	F=0.0862, p=0.9177
Week 4	0.50 \pm 0.02	0.48 \pm 0.02	0.45 \pm 0.02	F=0.9800, p=0.3866
Week 6	0.41 \pm 0.01	0.43 \pm 0.01	0.43 \pm 0.01	F=0.4931, p=0.6154
Week 8	0.36 \pm 0.02	0.37 \pm 0.02	0.40 \pm 0.03	F=1.6165, p=0.2172
Week 10	0.48 \pm 0.01	0.46 \pm 0.02	0.47 \pm 0.01	F=0.3581, p=0.7018
Week 12	0.41 \pm 0.02	0.39 \pm 0.01	0.39 \pm 0.01	F=0.2598, p=0.7728
Week 14	0.40 \pm 0.02	0.42 \pm 0.01	0.40 \pm 0.01	F=0.8798, p=0.4247
Week 16	0.45 \pm 0.02	0.37 \pm 0.02	0.45 \pm 0.02	F=4.5844, p=0.0175

DECLARATION OF AUTHORSHIP

I hereby declare that the present thesis, apart from the consultation of my supervisors, was completed independently by me, while no other than the stated sources and aids were used.

Furthermore, this thesis has not been presented elsewhere as a final assignment. The submitted written version is identical to the electronic version.

Huajing Yan

Nakhon Ratchasima, Thailand

16 May 2016